# The Role of Apoptosis Inducing Factor In modulating mtDNA copy number

Dissertation

zur

Erlangung des Doktorgrades (Dr. rer. nat.)

der

Mathematisch-Naturwissenschaftlichen Fakultät

der

Rheinischen Friedrich-Wilhelms-Universität Bonn

vorgelegt von

**Katharina Meyer**

aus

Lengerich

Bonn, Januar 2015

Angefertigt mit Genehmigung der Mathematisch-Naturwissenschaftlichen Fakultät der Rheinischen Friedrich-Wilhelms-Universität Bonn

1. Gutachter: Prof. Dr. Pierluigi Nicotera

2. Gutachter: Prof. Dr. Michael Hoch

Tag der Promotion: 08.05.2015
Erscheinungsjahr: 2015

## Summary

Mitochondrial DNA (mtDNA) encodes essential components of the mitochondrial electron transport chain. Depletion and mutations of mtDNA cause mitochondrial dysfunctions resulting in numerous human diseases, including neurodegeneration and mitochondrial disorders. However, despite extensive research, mechanisms that control mtDNA copy number are largely unknown.

The present study demonstrates that Apoptosis Inducing Factor (AIF), a mitochondrial protein with a dual role in cell-death and mitochondrial maintenance, is involved in the regulation of mtDNA. AIF deficiency resulted in a significant, several-fold increase of mtDNA copy number and this effect was evolutionary conserved among species. AIF regulates mtDNA copy number independently of previously described mechanisms controlling mtDNA content, including the activity of key mtDNA replication proteins, mitochondrial fusion, fission and biogenesis. However, inhibition of the cell cycle regulator CYE-1/cyclin E and the DNA damage response kinase ATL-1/ATR abrogated the effect of AIF deficiency on mtDNA copy number.

These findings provide new insights into the physiological functions of AIF and the regulatory pathways controling mtDNA quantity. As AIF as well as mtDNA dysregulation causes severe mitochondrial disorders in humans, this study extends our knowledge of molecular mechanisms underlying these pathologies and thereby may contribute to the development of novel therapeutic targets.

## Table of Content

# 1. Introduction

## 1.1. Mitochondria

Mitochondria are small dynamic organelles present in all eukaryotic cells. They are often referred to as the powerhouses of the cell because their main function is the production of adenosine triphosphate (ATP). ATP is the cells main energy source given that nearly every cellular activity is powered by the hydrolysis of ATP to adenosine diphosphat (ADP). Mitochondria produce ATP by oxidative phosphorylation (OXPHOS), which takes place along several protein complexes termed the electron transport chain (ETC). Mitochondria originated from an ancestral alpha-proteobacterial endosymbiont and due to this bacterial origin, they still contain and express their own genome. Mitochondrial DNA (mtDNA) encodes for only a few, but very essential proteins of the mitochondrial OXPHOS system.

Apart from cellular respiration, mitochondria acquired several additional functions during the course of evolution. They contribute to the production of amino acids and fatty acids, and regulate cellular levels of metabolites and cofactors of various enzymes. Moreover, by controlling apoptosis, a very important programmed cell death pathway, mitochondria are indispensable for the regulation of development (Newmeyer et al., 1994). Finally, mitochondria are critical for metal metabolism by synthesizing heme and Fe-S clusters (Lill and Muhlenhoff, 2008) and participate in $Ca^{2+}$ homeostasis (De Stefani et al., 2011).

Since mitochondria serve a variety of cellular functions, their progressive impairment plays a pivotal role in the ageing process (Miquel et al., 1980, Gkikas et al., 2014). Moreover, mitochondrial dysfunction contributes to several neurodegenerative diseases and causes an array of very heterogeneous human diseases, termed mitochondrial disorders (Koopman et al., 2013). Mitochondrial disorders are the consequence of mutations of nuclear and mitochondrial genes encoding for proteins important for mitochondrial maintenance or the OXPHOS system. Although these mutations can either be present on nuclear or mitochondrial genes, the primary cause of mitochondrial disorders are mtDNA mutations or impairments of mtDNA maintenance proteins (Taylor and Turnbull, 2005, Schapira, 2012). Consequently, increasing our knowledge on mtDNA

regulation and maintenance is crucial for the treatment of mitochondrial disorders and its detrimental effects on human health.

### 1.1.1. Mitochondrial Structure

Mitochondria are double membrane organelles organized into five distinct but functionally connected areas: outer mitochondrial membrane (OM), intermembrane space (IMS), inner mitochondrial membrane (IM), cristae and matrix.

The OM secludes mitochondria from the cytosol and contains integral membrane proteins ensuring the transport of molecules and proteins. One such integral OM protein is the translocase of the outer membrane (TOM) complex, an essential transporter for mitochondrial pre-proteins (Ryan et al., 2000).

The IMS comprises an aqueous compartment between the two mitochondrial membranes. Many intermembrane space proteins play an important role in coordinating mitochondrial function with cellular processes by connecting mitochondrial signaling cascades with the cytosol. The IM participates in several processes: firstly, several transport processes between the IMS and the matrix are regulated by integral IM proteins. For instance, the inner membrane translocase (TIM) complex actively transports mitochondrial proteins into the matrix. Additionally, several transport proteins catalyze the transport of metabolites across the IM, thereby linking metabolic pathways in the cytosol to the mitochondrial matrix (Wohlrab, 2009). Secondly, proteins essential for mediating fusion events, such as optic atrophy-1 (OPA1) are located in the IM. Thirdly and most importantly, the ETC is located in the IM. To increase the integration surface for ETC components the IM forms invaginations, termed cristae.

Metabolic processes necessary to fuel the OXPHOS system, such as the citric acid cycle and oxidation of fatty acids occur in the matrix. In addition, in this compartment the mitochondrial genome is maintained, replicated, transcribed and translated.

In mammalian cells mitochondria are organized in a dynamic interconnected network that undergoes constant morphological changes through mitochondrial fusion and fission processes (Youle and van der Bliek, 2012). Increased fusion leads to an elongated mitochondrial network and increased fission results in its fragmentation. Mitochondrial fusion is facilitated by three dynamin related

GTPases (Mitofusin 1 (Mfn1), Mitofusin 2 (Mfn2) and OPA-1) (Song et al., 2009) while mitochondrial fission is catalyzed by the dynamin realted protein 1 (DRP1). The antagonistic activities of mitochondrial fusion and fission are required to maintain form and function of mitochondria, including mitochondrial distribution and inheritance, coordination of cell death programs or adaption to bioenergetic requirements. For instance, increased mitochondrial fusion under starvation conditions protects the organelle from degradation and maximizes energy production (Gomes et al., 2011, Rambold et al., 2011). In addition, fusion and fission processes are crucial to maintain mitochondrial quality (Youle and van der Bliek, 2012). For instance, mitochondrial fusion represents an important mechanism for respiratory active cells to exchange mitochondrial content, such as metabolites, enzymes, mitochondrial gene products and mtDNA (Nakada et al., 2009). This functional complementation is especially important for an equal distribution of damaged and functional mtDNA molecules. This heteroplasmy is critical for maintaining a functional organelle (Nakada et al., 2009). Conversely, mitochondrial fission maintains mitochondrial quality by facilitating mitophagy, the degradation of defective mitochondria via autophagy (Twig et al., 2008, Kageyama et al., 2012, Kageyama et al., 2014). Thus, balanced fusion and fission events maintain a functional organelle and disruption of one of these processes has severe consequences. For instance, decreased mitochondrial fusion by conditional deletion of Mfn1 and Mfn2 leads to mtDNA depletion and mitochondrial dysfunction (Chen et al., 2010) while mutations of OPA1 lead to the development of optic atrophy in humans, a progressive loss of retinal ganglion cells (Liesa et al., 2009).

### 1.1.2. Oxidative Phosphorylation (OXPHOS) and Electron Transport Chain (ETC)

Hydrolysis of ATP to ADP is the major source of transferring free energy within a cell. The process by which ADP is phosphorylated to form ATP is termed oxidative phosphorylation (OXPHOS). The OXPHOS system is comprised of five protein complexes forming the electron transport chain (ETC), which represents the basis for mitochondrial ATP production. The transfer of electrons from nicotinamide adenine dinucleotide (NADH) or flavin adenine dinucleotide (FADH2) to molecular oxygen generates the energy to phosphorylate ADP. This reaction takes place along with electron transport through the ETC, which is composed of four oxidoreductase complexes and the ATP

synthase complex: the NADH dehydrogenase (complex I or CI), succinate dehydrogenase (complex II or CII), cytochrome c reductase (complex III or CIII) and cytochrome c oxidase (complex IV or CIV). Additionally, two electron carriers ubiquinone and cytochrome c (Cyt c) shuttle electrons along the respiratory chain. Ubiquinone transfers electrons from CI/CII to CIII and Cyt c from CIII to CIV. The series of redox reactions is coupled to the transfer of protons across the IM. This leads to the buildup of a proton concentration gradient between the matrix and the IMS and an electrochemical potential across the IM. This membrane potential is utilized by the F0F1-ATPase (complex V or CV) to couple the reflux of protons into the matrix with the phosphorylation of ADP to generate ATP. In addition, the mitochondrial membrane potential is required for additional mitochondrial functions, such as uptake of the signaling molecule $Ca^{2+}$ (Rottenberg and Scarpa, 1974), transport of metabolites across the IM (Eilers et al., 1987), stabilization of mtDNA translation products (Cote et al., 1990) and initiation of apoptosis (Zamzami et al., 1995). Therefore the membrane potential serves as a marker for mitochondrial function.

The protein complexes of the ETC are organized into different supercomplexes or respirasomes. The most stable supercomplexes in mammals are the dimeric ATP synthase and the $CI/CIII_2/CIV_{1-4}$ supercomplex, comprising CI, dimeric CIII and one to four copies of CIV. The organization into respirasomes has functional importance since it allows enhanced transfer rates (termed electron channeling) as well as regulation and increased stabilization of the OXPHOS complexes. Furthermore, supercomplexes determine the ultrastructure of the IM. The oligomerisation of the ATP synthase in the IM induces a strong local bending of the membrane, which results in the formation of cristae structures and increases the area for the integration of ETC components (Schagger et al., 2004, De los Rios Castillo et al., 2011).

## 1.2. Mitochondrial DNA (mtDNA)

The ETC comprises 90 proteins encoded by both the nuclear and mitochondrial genome (see Table 1-1). All of the 13 mtDNA-encoded proteins are essential parts of the ETC and the ATP synthase complex. Consequently, alterations of mtDNA severely impact mitochondrial OXPHOS.

**Table 1-1:** Overview of ETC subunits encoded by mitochondrial DNA (mtDNA) and nuclear DNA (nDNA)

| | Complex I | Complex II | Complex III | Complex IV | Complex V |
|---|---|---|---|---|---|
| mtDNA | 7 | 0 | 1 | 3 | 2 |
| nDNA | 39 | 4 | 10 | 10 | 14 |

MtDNA is circular double stranded DNA located in the matrix of mitochondria. Eukayotic cells typically contain thousands of mtDNA molecules (Malka et al., 2006) (See Figure 1-1).

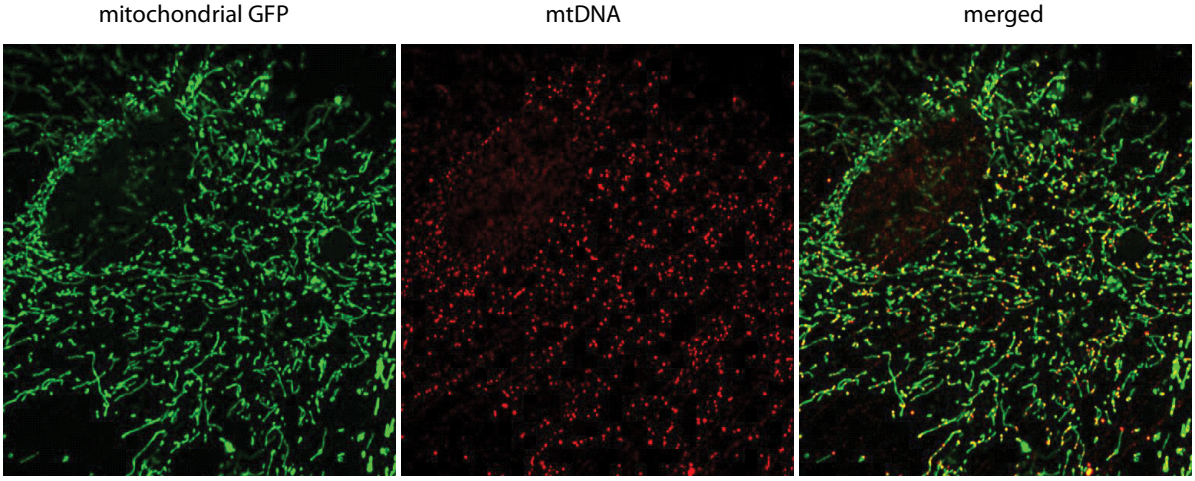


**Figure 1-1: Confocal images of mitochondria and mtDNA in mouse embryonic fibroblast (MEF) cells.** MEF cells expressing GFP targeted to mitochondria (left) were immuno-stained with anti-DNA antibodies to visualize mtDNA molecules (middle).

In contrast to its nuclear counterpart, mammalian mtDNA is very small with an approximate length of 16 kilobases (kb). The mitochondrial gene structure is very compact and the coding region of 13 proteins, 22 transfer RNAs (tRNAs) and 2 ribosomal RNAs (rRNAs) contains no introns. The only non-coding region of mtDNA is termed the displacement loop (D-loop), which contains the regulatory sequences for transcription and replication. Replication and segregation of mtDNA is radically different from the nuclear genome since mtDNA is constantly replicated in the mitochondrial matrix, independently of the cell cycle (Falkenberg et al., 2007). The mitochondrial genome is maternally inherited, paternal mitochondria and mtDNA are actively destroyed after fertilization (Sutovsky et al., 1999, Nishimura et al., 2006, Al Rawi et al., 2011). Due to this unique feature, mtDNA

is a powerful tool for tracking ancestry within species and frequently used in genealogy and anthropology research.

In contrast to the nuclear genome, mtDNA lacks histones but several associated proteins pack mtDNA into dense structures, termed nucleoids. Mitochondrial nucleoids facilitate a variety of functions, including organization and protection of mtDNA. During mtDNA replication, repair and translation, several ancillary factors are recruited, which render nucleoids very dynamic structures. Consequently, the protein repertoire is not entirely characterized (Bogenhagen, 2012). The most abundant nucleoid protein is the mitochondrial transcription factor A (TFAM) (Hallberg and Larsson, 2011, Shi et al., 2012), which represents the main mtDNA packaging factor and plays a crucial part in mtDNA transcription and replication. In addition, several other proteins comprising the mtDNA repair and replication machinery are localized to nucleoids in mammals, including DNA polymerase γ, Twinkle or the single stranded mtDNA binding protein (mtSSBP) (Bogenhagen, 2012).

The 13 proteins encoded by mtDNA are critical for mitochondrial function as they are rate-limiting for ETC assembly. The assembly of the ETC is very complex and requires a tightly regulated and coordinated expression of nuclear and mitochondrial genes. Accordingly, mutations of distinct accessory proteins that regulate mtDNA maintenance, transcription and replication lead to ETC impairments with severe pathological consequences in humans. Apart from mtDNA quality, reduction of mtDNA copy number leads to the clinically very heterogeneous mitochondrial depletion syndrome in humans (El-Hattab and Scaglia, 2013). Paradoxically, a severe increase in mtDNA copy number leads to nucleoid enlargement, age-dependent mtDNA deletions and ETC dysfunction in mice (Ylikallio et al., 2010). Therefore, maintaining an appropriate amount of functional mtDNA molecules is crucial for cell viability. In fact, quantitative or qualitative alterations of the mitochondrial genome are the primary cause of mitochondrial disorders (Taylor and Turnbull, 2005, Schapira, 2012, Koopman et al., 2013).

Consequently, the identification of proteins involved in regulation and maintenance of mtDNA is helpful for the understanding and treatment of mitochondrial dysfunction.

## 1.3. Mitochondria in Ageing, Neurodegeneration and Pathology

Since mitochondria are critical for various cellular processes it is not surprising that dysfunction of this organelle can lead to a myriad of human pathologies. Progressive impairments of mitochondrial function, including increased oxidative damage and decreased antioxidant defense are thought to contribute substantially to biological ageing. In fact, mitochondria from aged subjects show reduced oxidative phosphorylation and ATP production as well as increased production of reactive oxygen species (ROS) (Gomez et al., 2009, Gouspillou et al., 2014, Sgarbi et al., 2014). Conceptually, the mitochondrial theory of ageing considers ageing a vicious cycle of accumulating oxidative damage to proteins, lipids, nuclear DNA and mtDNA over time. Increased oxidative damage, in particular to mtDNA, causes ETC impairments, consequently increased ROS production and further oxidative damage to DNA. However, this is a simplified view on the role of mitochondria in ageing.

For instance, mice with mutated polymerase γ (POLG) (POLG mutator mice) and therefore a defective proofreading capacity during mtDNA replication, show a high mtDNA mutation rate and a premature ageing phenotype (Edgar and Trifunovic, 2009). Similarly, in ageing humans the mutation rate of mtDNA is up to 15-fold higher than that of nuclear DNA (Short et al., 2005). Interestingly, the mutator mice did not show increased ROS production, indicating that OXPHOS impairment rather than ROS might be responsible for the ageing phenotype (Trifunovic et al., 2005). However, other evidence indicates that mitochondrial dynamics as well as impaired cellular protein homeostasis contribute also to the very complex ageing process (Douglas and Dillin, 2010, Gkikas et al., 2014, Sgarbi et al., 2014).

Disruption of a variety of mitochondrial functions, such as loss of respiratory activity, mtDNA mutations, defects in mitochondrial degradation, impaired mitochondrial dynamics, altered structure and morphology as well as reduced mitochondrial trafficking and transport, either contribute or cause neuronal demise (Parashos et al., 2014). Consequently, mitochondrial dysfunctions are a key component in the pathology of late-onset, progressive neurodegenerative diseases, including Parkinson`s, Huntington`s, Alzheimer`s, amyotrophic lateral sclerosis or Charcot-Marie-Tooth, which are clinically characterized by impairments of motor functions, cognitive decline as well as alterations in behavior and personality.

An additional class of genetically very diverse human pathologies caused by mitochondrial dysfunction are the so-called mitochondrial disorders. These disorders are generally divided into two

classes. Secondary or acquired disorders manifest from accumulation of mitochondrial damage over time. They can either directly cause several well-defined neuromuscular syndromes or indirectly contribute to other degenerative disorders such as diabetes, cancer or cardio-vascular diseases.

In contrast, primary or inherited mitochondrial disorders are either caused by reduction of mtDNA copy number or mutations of mtDNA and nuclear DNA. The onset of these diseases varies between birth and late adulthood and they are characterized by a very heterogeneous combination of symptoms. Therefore, they are further classified either by the resulting biochemical defects or their clinical manifestation. Biochemical defects include defects in the ETC, in pyruvate-oxidation, fatty-acid metabolism or the Krebs cycle. Accordingly, tissues with high-energy expenditure such as muscle, brain and retina are most vulnerable to changes in mitochondrial function, even though also tissues with a lower metabolic demand are affected, including peripheral nerves, sensory organs, heart, kidneys and endocrine tissues (DiMauro, 2004). Consequently, the most common pathological phenotypes of mitochondrial disorders are vision impairments, neuronal degeneration and muscular atrophy, which are associated with a variety of clinical syndromes (Schapira, 2012). For example, chronic progressive external ophthalmoplegia (CPEO) describes a late onset, progressive inability to move eyes or eyebrows, which in severe cases can extend to cognitive impairment or growth retardation. The Kearns-Sayre-Syndrome (KSS) describes CPEO with an additional degeneration of the retina, cardiomyopathy and can also include cerebellar ataxia and muscle weakness. Patients suffering from myoclonic epilepsy with ragged red fibres (MERRF) syndrome experience myoclonic seizures, clumping of damaged mitochondria in the subsarcolemmal region of muscle fibres, hearing loss and exercise intolerance. The clinical manifestation of mitochondrial encephalomyopathy, lactoacidosis and stroke like episodes is defined as the MELAS syndrome while patients with the LHON syndrome (Lebers hereditary optic neuropathy) show degeneration of retinal ganglion cells. Leigh´s disease is a neurometabolic disorder of the CNS and combines several phenotypes such as dysphagia, seizures, muscle atrophy, ataxia and respiratory failure (Koopman et al., 2013).

In this context, a mitochondrial disorder similar to Leigh´s disease has been associated with the mitochondrial protein apoptosis inducing factor (AIF) (Ghezzi et al., 2010). Patients carrying the AIF-R201 deletion display delayed psychomotor development, severe muscle atrophy and progressive neurodegeneration. Furthermore, reduction of AIF protein levels leads to mitochondrial CI deficiency in mice (Vahsen et al., 2004, Benit et al., 2008). These “harlequin” mice (see section 1.4.4) display many

features of human Leigh´s syndromes, such as progressive neurodegeneration, ataxia and muscle atrophy.

Despite considerable progress in understanding the causes of mitochondrial disorders no effective treatments have been developed so far (Benit et al., 2008). This can be partially attributed to the lack of suitable animal models. However, the discovery of the harlequin mouse offered a valuable *in vivo* model to identify the underlying molecular mechanisms of mitochondrial disorders and to design treatments for such diseases.

## 1.4. Apoptosis Inducing Factor (AIF)

AIF is a flavoprotein with an oxidoreductase activity, located in the IM, IMS or OM of mitochondria (Susin et al., 1999, Yu et al., 2009). Under stress conditions AIF is cleaved and translocated to the nucleus where it assists in chromatin condensation and DNA degradation (Joza et al., 2001) (see Figure 1-2). This cell death signaling event occurs in a caspase-independent manner. Beyond its role in cell-death, AIF is essential for cell survival, implicated in the maintenance of mitochondrial morphology and involved in cellular energy metabolism by stabilizing the ETC, in particular CI (Vahsen et al., 2004) (see Figure 1-2). This dual role of AIF in cell death and survival is highly evolutionary conserved from nematodes, such as *C. elegans*, to mice and humans.

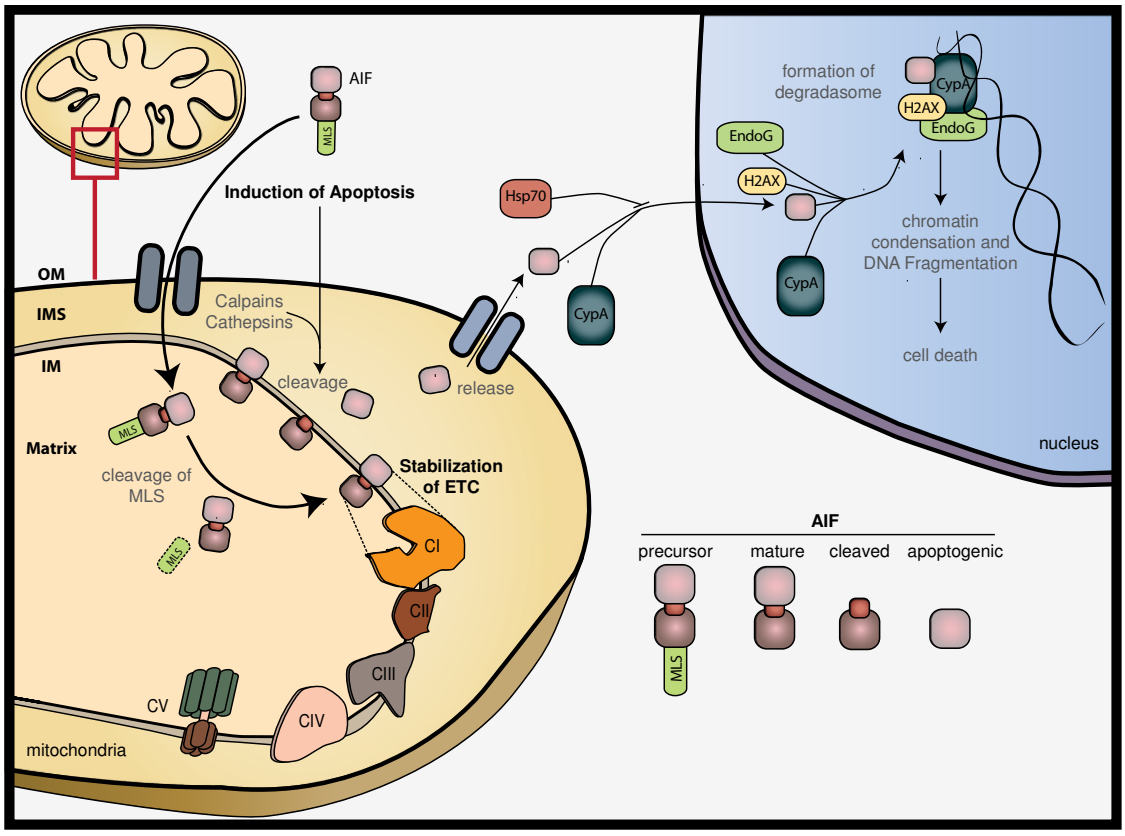


**Figure 1-2: Schematic overview of AIF functions in cell survival and apoptosis.** The AIF precursor protein is imported into the mitochondria via its mitochondrial localization sequence (MLS). The MLS is cleaved and mature AIF is integrated into the inner mitochondrial membrane (IM). AIF is important for stabilization of the electron transport chain (ETC) in non-apoptotic conditions. Induction of apoptosis leads to the proteolytic processing of AIF by calpains/cathepsins and apoptogenic AIF is released from mitochondria. Translocation to the nucleus is inhibited by Hsp70 and enhanced by CypA. In the nucleus, AIF recruits CypA, H2AX and EndoG to form the degradasome, which leads to chromatin condensation and DNA fragmentation. OM: outer mitochondrial membrane, IMS: intermembrane space

### 1.4.1. Discovery of AIF

In the early 1990s little was known about the molecular mechanisms underlying programmed cell death (PCD) and it was shown that cells lacking a nucleus (anucleate cells) had the capability to undergo PCD (Schulze-Osthoff et al., 1994). Therefore, the hypothesis that cytoplasmic factors might control apoptosis arose. A first breakthrough was the observation that the protein B-cell lymphoma 2 (Bcl2) protected cells from PCD (Allsopp et al., 1993, Jacobson et al., 1994, Newmeyer et al., 1994). Moreover, it was shown that reduction of the mitochondrial transmembrane potential preceded the first signs of nuclear apoptosis, such as chromatin condensation and DNA fragmentation (Zamzami et al., 1995). Therefore, in 1996 the group of Guido Kroemer tried to link mitochondrial dysfunction to

apoptosis. They found that mitochondria control nuclear apoptosis by the opening of the mitochondrial permeability transition pore (MPTP), which is localized at the OM, and that this opening is a critical event in inducing PCD (Zamzami et al., 1996). Permeabilization of the OM leads to the release of soluble factors, which alone can force the nucleus to adopt an apoptotic-like morphology even in a cell-free system (Zamzami et al., 1996). Only six months later one of these factors was purified and named Apoptosis Inducing Factor (AIF) (Susin et al., 1996).

### 1.4.2. AIF in Apoptosis

PCD is the mechanism of cellular self-destruction and is critical for a variety of normal physiologic processes, such as tissue maintenance by removal of defective cells and development. PCD can be classified into four different types.

The key hallmark of type 1 PCD, termed apoptosis, is the activation of caspases, a specific class of cysteine proteases. Induction of apoptosis is achieved by the activation of "death receptors" in an "extrinsic" pathway or via a mitochondria dependent "intrinsic" pathway (Portt et al., 2011). The intrinsic pathway is associated with the permeabilisation of the OM and the release of several pro-apoptotic proteins from the IMS. For instance, the release of Cyt c leads to a direct activation of caspases, while Smac/DIABLO (Second Mitochondrial derived activator of Caspase/Direct IAP-Binding protein with a Low pI) and the serine protease Omi/HtrA2 antagonize caspase inhibitors (Hengartner, 2000). The activation of caspases ends in well-known hallmarks of apoptosis such as DNA and nuclear fragmentation or membrane blebbing.

Type 2 PCD is morphologically characterized by the appearance of "autoplasmic" double membrane vacuoles and therefore termed autophagic PCD. This mode of PCD is characterized by massive degradation of essential organelles by lysosomal activity (Gozuacik and Kimchi, 2007).

Type 3 PCD is morphologically characterized by the appearance of swelling organelles and fragmentation of the plasma membrane (Schweichel and Merker, 1973).

Given that PCD type 2 and 3 occur without pronounced chromatin condensation and independently of caspase activation they are classified as necrosis-like (Leist and Jaattela, 2001).

Induction of type 4, apoptosis-like PCD results in chromatin condensation similar to apoptosis without activation of caspases (Jaattela and Tschopp, 2003). This cell death pathway is controlled by mitochondria and its main effector is AIF.

Under physiological conditions AIF is anchored to the IM by an integral membrane domain. In response to apoptotic stimuli AIF is cleaved by calpains or cathepsins and soluble AIF protein is released into the IMS (Polster et al., 2005, Yuste et al., 2005, Liu et al., 2009). Upon permeabilization of the OM, soluble AIF is released from mitochondria and translocated to the nucleus (see Figure 1-2). This translocation is positively regulated by cyclophilin A (CypA) while it is inhibited by the heatshock protein Hsp70 (Gurbuxani et al., 2003, Doti et al., 2014). In the nucleus AIF induces a whole pattern characteristic of nuclear apoptosis, including chromatin condensation and DNA fragmentation (Susin et al., 1996, Susin et al., 1999). Interestingly, AIF alone does not possess DNAse activity and AIF-mediated DNA degradation depends on the recruitment of downstream nucleases. Studies in *C. elegans* demonstrated that the worm AIF ortholog WAH-1, cooperates with the mitochondrial endonuclease CPS-6/endonuclease G (EndoG) to promote DNA degradation (Wang et al., 2002). Moreover, in alkylating DNA damage-induced necroptosis, the process of programmed necrosis, AIF participates in assembling a DNA degradation complex with histone H2AX and CypA (Artus et al., 2010) (see Figure 1-2).

Strikingly, the C-terminal domain of AIF, is responsible for the pro-apoptotic function and shows a strong homology to bacterial NADH ferredoxin reductases or NADH-oxidoreductases from other vertebrates (*Xenopus laevis*) and in-vertebrates (*C. elegans*, *D. melanogaster*), but also with dehydroascorbate reductases in plants (Lorenzo et al., 1999). Albeit, AIF shows an oxidoreductase activity, it can be dissociated from its pro-apoptotic function (Susin et al., 1999, Miramar et al., 2001, Vahsen et al., 2004, Cheung et al., 2006). Paradoxically, conditional AIF knockout mice show increased apoptosis and AIF is not important for apoptosis during early embryonic development (Brown et al., 2006). AIF deficient embryos show a similar-to-wildtype morphology until embryonic day E7.5 and a normal developmental cavitation process, but extensive cell death occurs at day E9, which immediately results in embryonic lethality. This extensive abnormal cell death was caused by reduction of mitochondrial CI and therefore impairments of the energy metabolism (Brown et al., 2006). However, several *in vivo* studies suggest that AIF is required for PCD after certain types of neuronal injury, such as hypoxia-ischemia (Klein et al., 2002, Cheung et al., 2005, Sun et al., 2012).

### 1.4.3. Structure of AIF

AIF is a mitochondrial protein that is transcribed in cytoplasmic ribosomes and transported into mitochondria via a N-terminal localization sequence (MLS). This precursor protein contains two nuclear localization sequences (NLS) and a NAD- and FAD binding motif (see Figure 1-3).

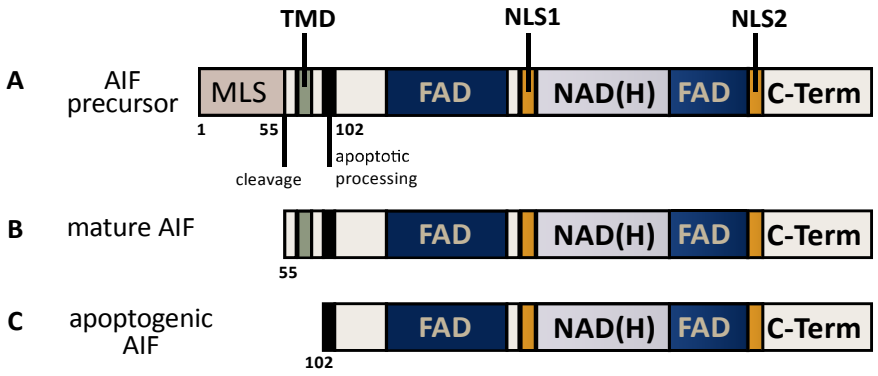


**Figure 1-3:** Overview of the AIF protein structure. **A** The AIF precursor is translated in the cytosol and transported to mitochondria via its mitochondrial localization sequence (MLS). It contains one transmembrane domain (TMD) and two nuclear localization signals (NLS). **B** Structure of mature AIF after cleavage of the MLS. **C** After cleavage of the TMD AIF becomes apoptogenic.

After cleavage of the MLS, AIF binds FAD, which is the only identified prosthetic group and is necessary for correct protein folding (Miramar et al., 2001, Mate et al., 2002). This mature form of AIF is finally integrated into the IM with its major part presumably facing the IMS (see Figure 1-3). Under physiological conditions native AIF appears predominantly in a monomeric form but dimerizes upon binding of NADH and subsequent reduction of the flavin moiety (Ferreira et al., 2014).

Analysis of the crystal structure of the mature mouse AIF (Δ1-121) revealed that it functions as an electron transferase with a mechanism similar to bacterial ferredoxin reductases (Mate et al., 2002). The same study showed that its overall structure displays a glutathione reductase (GR)-like fold. Similar to these enzymes AIF has three functional domains: The FAD binding domain (residues 122-262 and 400-477), a NAD(H)-binding domain (263-399) and a C-terminal domain (478-610). Moreover, an exclusive feature of mammalian AIF is the existence of a proline (P), glutamic acid (E), serine (S) and threonine (T) rich (PEST) sequence. PEST sequences are important for a rapid protein turnover and protein-protein interactions. In addition, this sequence contains a Pro-rich motif (PPSAPAVPQVP) with a polyproline-2 helix that suggests a possible interaction between AIF and proteins containing SH3 and WW modules (Mate et al., 2002). In fact, this proline-rich domain is

fundamental for chromatinolysis, as it mediates the association with histone H2AX during caspase-independent cell death (Artus et al., 2010). The crystal structure of human AIF proved to be quite similar to the mouse structure (Ye et al., 2002). However, it bears a strong positive electrostatic surface potential, which results in sequence- and length- independent binding of AIF to DNA (Ye et al., 2002). Another very recent structural analysis of human AIF identified a second NAD(H) binding site with *in vivo* relevance (Ferreira et al., 2014). In fact, this site is important for proper dimerisation of AIF, and two out of three detected human pathologies caused by AIF dysfunction show defects in this sequence (Ferreira et al., 2014).

### 1.4.4. AIF in Cell Survival

AIF is not a universal cell death effector and during recent years it has been recognized that AIF is a critical pro-survival factor. Given that a homozygous AIF knockout in mice results in embryonic lethality, the generation of conditional mouse models offered important tools to gain insights into the critical role of AIF in cell survival. One of the most relevant mouse models is the harlequin mouse. These animals show 80% reduced AIF protein expression caused by a pro-viral insertion in the AIF gene (Klein et al., 2002). Both harlequin males and females are viable and do not show any obvious phenotypes during early adulthood (Klein et al., 2002, Benit et al., 2008) . However 2-3 month after birth these mice show hair loss, develop ataxia and exhibit retinal degeneration. Furthermore, harlequin mice show progressive cerebellar degeneration after 4 months of age (Klein et al., 2002). In general, AIF reduction has a detrimental effect on the health of ageing adult mice (Benit et al., 2008). These phenotypes are caused by mitochondrial dysfunction induced by ETC deficiency (Vahsen et al., 2004, Chinta et al., 2009). The harlequin mouse offers therefore, a suitable *in vivo* model for studying human mitochondrial disorders because it resembles several pathological phenotypes of these diseases (Benit et al., 2008).

*AIF and Mitochondrial Respiration*

A variety of experimental evidence suggests that AIF is crucial for mitochondrial respiration and metabolism, both necessary for cell survival.

The first observations of broad metabolic changes connected to AIF were made in AIF knockout embryonic stem cells (ESCs) by Vahsen and colleagues (Vahsen et al., 2004). This study showed that $AIF^{-/-}$ ESCs exhibit reduced in vitro growth and enhanced lactate production, due to 50% reduced activity of CI and CIII. Moreover, the $AIF^{-/-}$ ESCs displayed no oxidative stress-induced damage but enhanced glucose dependency. The same study demonstrated alterations of CI protein levels in the harlequin mouse (Vahsen et al., 2004). While loss of CI subunits was detectable in all organs of harlequin mice, loss of CI activity was observed mainly in the central nervous system including cortex, cerebellum, thalamus, optical nerves and retina as well as in skeletal muscle (Vahsen et al., 2004). Apart from CI, the absence of AIF can also affect other respiratory complexes. For instance, a targeted deletion of AIF in mouse heart or liver results in CI deficiency and abnormal CIV activity in both tissues, while loss of CV subunits only occurred in the liver (Joza et al., 2005, Pospisilik et al., 2007). These studies showed that AIF has an important function in stabilizing the ETC in mitochondria, even though the underlying mechanism of its stabilizing function remains enigmatic.

Another observed phenomenon of AIF deficiency is altered ROS production as a consequence of CI impairments. These studies on ROS and oxidative damage in conditions of reduced AIF protein expression showed, however, inconsistent outcomes. For instance siRNA knockdown of AIF in different cell lines, such as HCT116, DLD-1 and MCF-7 led to decreased ROS levels, suggesting that AIF is a ROS generator (Urbano et al., 2005). In contrast, studies in harlequin mice showed increased oxidative stress in the cerebellum as displayed by lipid peroxidation as well as increased glutathione and catalase activity, suggesting that loss of AIF increases ROS production (Klein et al., 2002). The latter findings were supported by detailed studies in Hep3B and HeLa cells, showing that knockdown of AIF leads to significantly increased ROS levels (Apostolova et al., 2006). Interestingly, studies in AIF deficient ESCs and mitochondria derived from heart- and liver-specific AIF knockout mice did not show any alterations in ROS production (Joza et al., 2005, Pospisilik et al., 2007).

Finally, AIF deficiency leads to complex metabolic consequences including decreased ATP, decreased NAD+ and increased adenosine monophosphate (AMP) levels as well as a metabolic switch towards glycolysis (Pospisilik et al., 2007). Mice carrying a muscle-specific deletion of AIF exhibit improved glucose tolerance and insulin sensitivity as well as resistance to diet induced obesity and diabetes (Pospisilik et al., 2007). This is even more pronounced in harlequin mice, which show an almost complete resistance to diet-induced diabetes (Joza et al., 2005, Pospisilik et al., 2007).

*AIF and Mitochondrial Morphology*

Mitochondrial metabolism is tightly linked to organelle structure and morphology. Apart from the role of AIF in mitochondrial ETC composition, there is evidence that AIF is also involved in regulating mitochondrial structure. First observations were made in a telencephalon-specific AIF knockout mouse model (*tel* AIFΔ), which lacks AIF only in cortical neurons (Cheung et al., 2006). Mitochondria in neurons from *tel* AIFΔ mice were fragmented with aberrant cristae, which were dilated and not oriented in an orderly fashion (Cheung et al., 2006). Moreover, overexpression of AIF anchored to the IM led to increased mitochondrial fusion in wildtype cells (Cheung et al., 2006). Notably, the evolutionary conserved fusion protein OPA1 was suggested to form a complex with AIF to cooperatively regulate and stabilize the ETC (Zanna et al., 2008). Additionally, harlequin mice cerebella showed reduced levels of Mfn1, suggesting that alterations of mitochondrial fusion led to cerebellar degeneration (Chung et al., 2011).

*AIF and Cell Division*

Upon the characterization of the harlequin mouse, AIF deficiency was for the first time considered to impact cell cycle and cell division. The cell cycle comprises four consecutive phases: a long growth phase (G1 phase), a DNA replication phase (S phase), a short growth phase (G2 phase) and finally cell division or mitosis (M phase). Klein and colleagues observed that postmitotic retinal neurons and cerebellar granule cells in harlequin mice re-enter the cell cycle and subsequently undergo apoptosis (Klein et al., 2002). Moreover, mice with a specific AIF knockout in the cerebellum (*en1* AIFΔ and *nestin* AIFΔ) showed an increased number of Pukinje cells in S-phase, which did not undergo mitosis during neurogenesis (Ishimura et al., 2008). Furthermore, the same study showed that the Purkinje cell precursors display a shorter G1-phase, enter S-phase prematurely, arrest in G2 and initiate caspase-dependent apoptosis. In contrast, the G1/S phase transition in cerebellar granule cell precursors of these mice was disrupted presumably because cells were arrested in G1 (Ishimura et al., 2008).

Harlequin mice suffer not only from neurodegeneration but also sarcopenia, a degenerative loss of skeletal muscles, resulting from a reduced satellite cell pool in muscle tissue. This is due to a delayed cell cycle entry of the harlequin satellite cells, resulting in a stalled activation of satellite cell precursors, which delays muscle regeneration (Armand et al., 2011).

### 1.4.5. AIF in Neurodegeneration

AIF deficiency i*n vivo* leads to neuronal death and neurodegeneration, due to ETC defects that cause decreased neuronal energy availability and presumably increased neuronal ROS production.

Harlequin mice exhibit a late onset retinal degeneration with a loss of ganglion and amacrine cells starting after 3 month of age, while all neuronal layers are affected by the age of 11 month (Klein et al., 2002, Benit et al., 2008). Moreover, the harlequin cerebellum shows a progressive degenerative phenotype (Klein et al., 2002). While the gross cerebellar morphology at 3 month of age appears similar, a large population of cerebellar neurons shows condensed nuclei already at 4 month (Klein et al., 2002). After 7 month of age the cerebellum is much smaller and most of the cerebellar granule cells (CGNs) are lost at 12 month of age, probably due to increased oxidative stress and cell cycle re-entry (Klein et al., 2002). Similarly, AIF ablation in the embryonic or early postnatal cerebellum results in hypoplasia due to disrupted Purkinje cell development, resulting from a premature entrance into S-phase during neurogenesis as well as S-phase cell cycle arrest and subsequent apoptosis of CGNs (Ishimura et al., 2008). Thus, AIF is required for cerebellar neurogenesis as well as for the survival of postmitotic cerebellar neurons. In addition, AIF is required for neuronal survival during cortical development since telencephalon-specific AIF knockout is lethal at the mouse embryonic day E17 (Cheung et al., 2006). Primary cortical neurons from these mice undergo PCD after two days in culture, which can be rescued by supplementation of additional pyruvate, uridine and glucose, suggesting impaired respiration as the cause of cell death (Cheung et al., 2006).

Although AIF appears to be a cell death inducer, there is evidence that the protein has also neuroprotective functions. In fact, AIF deficient harlequin mouse neurons show a striking resistance to NMDA- and kainic acid induced excitotoxicity (Klein et al., 2002, Cheung et al., 2005). Furthermore, reduced harlequin mice hippocampal neurons are protected against cell death evoked by kainic acid induced seizures (Cheung et al., 2005). AIF downregulation also reduced brain injury and increased neuronal progenitor cell survival after hypoxic-ischemia (Sun et al., 2012).

Overall, AIF acts as a Janus-like protein on neuronal survival. It can be either protective or harmful to neurons, depending on the neuronal type and the physiological conditions.

### 1.4.6. AIF in Human Pathology

There is recent evidence that AIF is associated with human mitochondrial disorders. To date three different pathological AIF mutations have been identified which lead to an early onset of neuromuscular symptoms and a considerably reduced lifespan in humans.

First, a deletion of the arginine residue R201 leads to severe mitochondrial encephalomyopathy, characterized by delayed psychomotor development, severe muscle atrophy, axonal sensory neuropathy, seizures and respiratory insufficiency (Ghezzi et al., 2010). This study showed reduced levels of respiratory CIII and CIV and almost depleted mtDNA content in muscle biopsies from affected patients. In addition, immortalized patient fibroblast cells showed decreased CI, CIII and CIV protein levels and a fragmented mitochondrial network (Ghezzi 2010). The residue R201 is part of the FAD-binding pouch and the second NAD(H)-binding site of AIF, which determine the protein´s conformational stability and dimerization status (Ghezzi et al., 2010, Ferreira et al., 2014). Upon AIF oxidation, R201 induces proper folding of the protein and limits the accessibility to the FAD-containing active site. Therefore, deletion of R201 perturbs the functional properties of oxidized/reduced AIF (Ghezzi et al., 2010). Upon exposure to NADH AIF-R201 can still form the FADH2-NAD charge transfer complex but its lifetime is considerably lower. Moreover, in contrast to wildtype AIF, oxidized AIF-R201 tends to lose the FAD cofactor (Ghezzi et al., 2010). As a functional outcome AIF-R201 displays an increased DNA binding affinity and induces increased sensitivity to staurosporine-induced cell death.

The second NAD(H) binding site is also affected in the recently reported AIF mutation E493V, which leads to Cowchock syndrome, an X-linked form of Charcot-Marie-Tooth disease, characterized by peripheral neuropathy, deafness and cognitive impairment (Rinaldi et al., 2012). An exchange of glutamine to valine at position 493 alters the electrostatic surface potential near the AIF redox-center, resulting in a four-fold higher reduction by NAD(H) and a significantly reduced half-life of the charge transfer complex (Rinaldi et al., 2012). The faster oxidation of AIF-NAD(H) increases the accumulation of monomeric AIF, which is more accessible to apoptotic cleavage (Rinaldi et al., 2012). Accordingly, patient fibroblast cells displayed no disturbances of respiratory complexes or ETC activity but had a higher nuclear translocation propensity for AIF-E493V and caspase-independent apoptosis (Rinaldi et al., 2012).

A third mutation of AIF, termed AIF-G308E, leads to an early prenatal ventriculomegaly, a brain malformation, characterized by an altered development of the intracranial architecture leading to abnormal tissue pressure and enlarged ventricles (Berger et al., 2011). Patients carrying the AIF-G308E mutation exhibit swallowing difficulties, seizures and muscle atrophy. Isolated mitochondria from muscle biopsies showed decreased CI and CIV activity (Berger et al., 2011).

The identification of several AIF mutations and their pathological sequelae have provided valuable insights into the pro-survival functions of AIF. Importantly, the general symptoms associated with these mutations are very similar to other mitochondrial disorders and therefore a better understanding of the physiological role of AIF might prove beneficial in treating mitochondrial diseases in the future.

## 2. Aims of this study

Mitochondria are essential for the function of cells, organs and whole organisms. Alterations of mitochondrial functions not only contribute to the ageing process but cause an array of human pathologies, such as neurodegenerative diseases, mitochondrial disorders, diabetes and cancer.

In this context, AIF plays a Janus-like role in cell survival. Although AIF is an evolutionary conserved pro-death factor, it is indispensable for mitochondrial function and AIF dysfunction leads to severe mitochondrial encephalomyopathy in humans.

Muscle biopsies from patients carrying the AIF-R201 mutation showed a depletion of mtDNA, suggesting that AIF is implicated in mtDNA maintenance (Ghezzi et al., 2010). Moreover, AIF was shown to directly interact with the mitochondrial endonuclease EndoG during PCD (Wang et al., 2002) and EndoG knockout mice display decreased mtDNA copy number in the heart (McDermott-Roe et al., 2011).

Considering these observations, I measured mtDNA copy number in harlequin mice and detected a significant increase in mtDNA content. Consequently, the present study aimed to elucidate the mechanism that led to increased mtDNA copy number in AIF deficient conditions. Initially, the study focused on well-established pathways that regulate mtDNA copy number by using *C. elegans* and harlequin mice as model systems. However, increased mtDNA copy number in AIF deficient conditions was independent of previously described mechanisms. Thus, I investigated pathways that are not primarily linked to the regulation of mtDNA copy number. Finally, the present study points to a new evolutionary conserved role of AIF in controling mtDNA copy number, mediated by the DNA damage response pathway and cell cycle regulators.

# 3. Results

## 3.1. Loss of WAH-1/AIF leads to increased mtDNA copy number and affects ETC composition at a posttranscriptional level

The following study takes advantage of two different model systems - the nematode *C. elegans* and the harlequin mouse model for addressing specific experimental questions. *C. elegans* was primarily used to study genetic interactions, due to its short life cycle, the availability of mutant strains and its feasibility for gene knockdown by RNA interference (RNAi). For knocking -down specific genes, nematodes were fed with bacteria containing the appropriate dsDNA construct. This approach was sufficient to reduce gene expression levels to residual 20-40%, which was confirmed in each experimental setting by measuring mRNA levels using quantitative real time PCR (qPCR).
The harlequin mouse was used as a mammalian model to confirm the results obtained in nematodes. These mice show 80% reduced AIF protein levels compared to wildtype littermates (Klein et al., 2002).

*Loss of WAH-1/AIF leads to an evolutionary conserved increase of mtDNA*

To assess whether AIF influences mtDNA copy number, I first measured mtDNA content in two different models of AIF deficiency. Treatment of *C. elegans* with *wah-1* RNAi for 12 days resulted in a significant, more than 2-fold increase of mtDNA molecules in nematodes (Figure 3-1 A). To assess whether this effect was evolutionary conserved, I measured mtDNA copy number in cerebella from harlequin mice and their wildtype littermates. Strikingly, harlequin mice cerebella showed a 4-fold increase of mtDNA in comparison to control littermates (Figure 3-1 A).

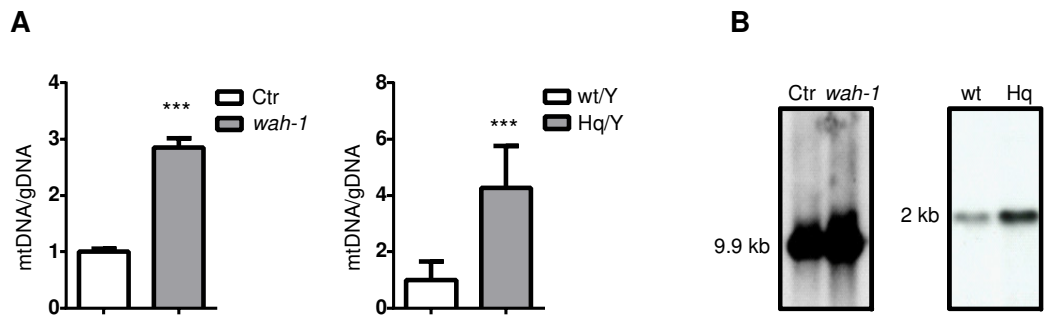


**Figure 3-1: Loss of WAH-1/AIF leads to an evolutionary conserved increase of mtDNA copy number in *C. elegans* and harlequin mice. A** qPCR and analysis of mtDNA copy number in N2 wildtype nematodes at day 12 (left). Worms were subjected to control and *wah-1* RNAi (n=5). (right) qPCR analysis of mtDNA copy number in wildtype (wt/Y) and harlequin mice (Hq/Y) cerebella at 6 month of age (n=5). Values represent fold difference relative to control conditions. Asterisks show statistical significance (unpaired Student´s *t*-test, *** $p < 0.001$). **B** Southern blot analysis showing mtDNA copy number in N2 wildtype nematodes at day 12 (left), subjected to control (Ctr) and *wah-1* RNAi. Southern blot analysis of mtDNA in wildtype (wt) and harlequin mice (Hq) cerebella at 6 month of age (right).

This increase of mtDNA was also present in other tissues derived from harlequin mice, including kidneys, lung, liver, testis and fat (data not shown). Next, I performed southern blot assays to verify whether the qPCR assay was detecting the full-length, functional mtDNA or mtDNA fragments. To this end, total DNA from nematodes after *wah-1* RNAi treatment and DNA from harlequin mice cerebella were processed and mtDNA was detected by using mtDNA-specific probes. Digestion of full-length mtDNA with restriction enzymes gave a fragment of 9.9 kb in *C. elegans* or a 2 kb fragment in mice (Figure 3-1 B). Southern blot analysis detected an increased amount of these fragments upon AIF deficiency in both, nematodes and mice (Figure 3-1 B). Together, these results demonstrate that loss of WAH-1/AIF leads to an increase of full-length mtDNA copy number, an effect that is evolutionary conserved.

*Increased mtDNA content does not lead to increased mitochondrial RNA expression*

Since loss of WAH-1/AIF led to an increase in mtDNA copy number, I asked next whether this elevation of mtDNA results in an increase of mtDNA gene expression. To this end, the mtRNA expression levels of several mtDNA-encoded genes including the CI-subunits ND1, ND4, ND4L, ND5, ND6, cytochrome B (Cyt B) as well as CIV-subunit COXI were measured by qPCR.

Interestingly, neither increased expression of ND1, ND4 and COXI in *C. elegans* (Figure 3-2 A) nor ND1, ND5, ND4L, CytB and COXI in harlequin mice was observed (Figure 3-2 B). Notably, also

expression of ND6 remained unchanged, indicating equal gene expression from light and heavy strand mtDNA promoters (Figure 3-2 B).

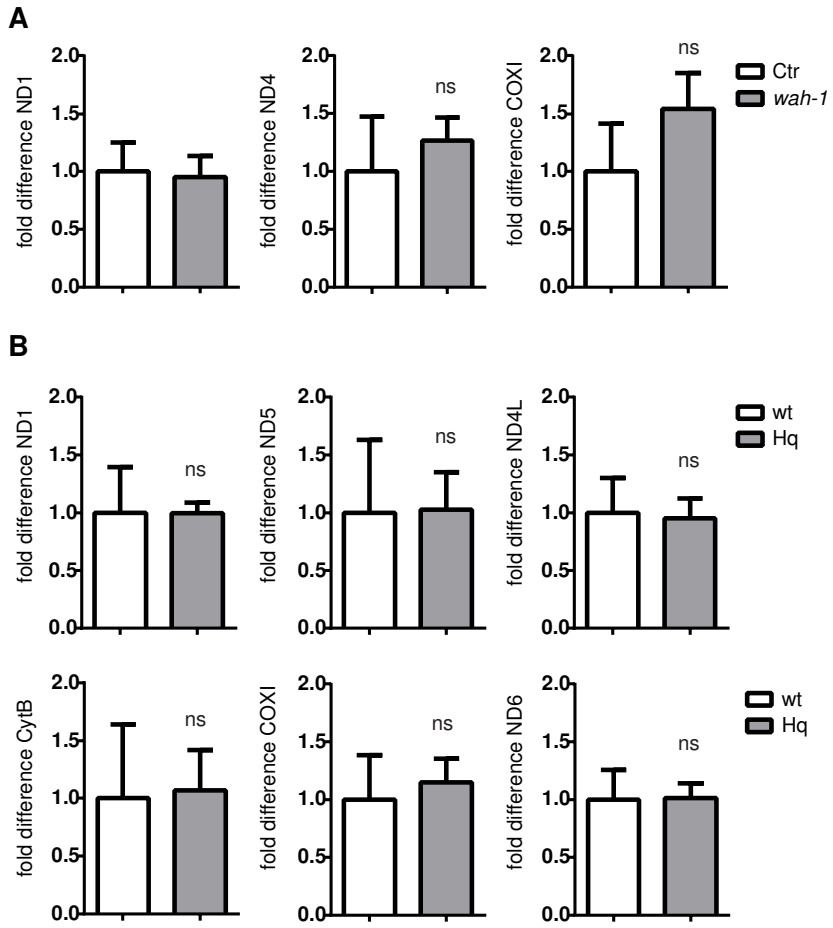


**Figure 3-2: Increased mtDNA copy number upon WAH-1/AIF deficiency does not lead to increased mtRNA. A** qPCR analysis of ND1, ND4 and COXI mRNA expression in *C. elegans* wildtype after treatment with control (C) or *wah-1* (W) RNAi. **B** Gene expression of ND1, ND5, ND4L, CytB, COXI and ND6 in cerebella from 6 month old wildtype (wt) and harlequin (Hq) mice. Values represent fold difference relative to control conditions (n=3). Asterisks show statistical significance (unpaired Student´s *t*-test, *** $p < 0.001$).

*Changes of ETC subunits occur at a posttranscriptional level*

During the past few years it was shown that loss of AIF leads to ETC deficiency due to loss of CI. For instance, harlequin mice show reduction of CI subunits in all tissues (Vahsen et al., 2004). Besides loss of CI, knockout of AIF in muscle or liver results in reduced levels of CIV (Joza et al., 2005) or CV (Pospisilik et al., 2007) respectively. However, these studies did not address whether ETC components

encoded by mtDNA and nuclear DNA are differentially expressed. Therefore, I assessed ETC composition in cerebella of 6 month old harlequin mice by western blot analysis using antibodies against different subunits encoded by nuclear DNA (nDNA) or mtDNA. The nDNA-encoded CI subunit Ndufb8 was robustly decreased while the mtDNA-encoded CI subunit ND5 showed no pronounced decrease in protein levels (Figure 3-3).

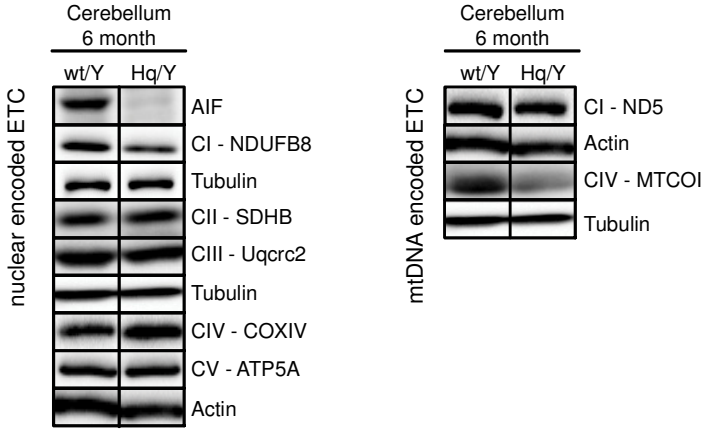


**Figure 3-3: AIF deficiency leads to posttranscriptional changes of ETC subunits A** Immunoblot analysis of nuclear-encoded proteins AIF, CI subunit NDUFB8, CII subunit SDHB, CIII subunit Uqcrc2, CIV subunit COXIV and CV subunit ATP5A (left). Western Blot analysis of mtDNA-encoded ETC subunits ND5 (CI) and MTCO1 (CIV) (right). Analysis was performed using samples from cerebella of 6 month old harlequin mice (Hq/Y) and control littermates (wt/Y) (n=5).

Interestingly, the nuclear encoded subunit of CIV (COXIV) was not changed while the mtDNA encoded subunit MTCO1 was decreased. In contrast, CII, CIII and CV subunits showed similar protein levels in wild type and harlequin mice (Figure 3-3). Thus, nuclear-encoded CI and mtDNA-encoded CIV were reduced in the cerebellum of harlequin mice. Given that the expression of mtDNA genes was normal upon AIF deficiency (Figure 3-2 B), this suggests a posttranscriptional effect of AIF on ETC subunits.

## 3.2. Increase of mtDNA copy number after WAH-1/AIF downregulation is not a consequence of ETC impairments or PGC1α activity

*Increase of mtDNA after loss of AIF is not a compensatory effect caused by ETC deficiency*

Several models of mitochondrial deficiency, including TFAM knockout mice and CI deficient nematodes, show increased mtDNA copy number and increased mitochondrial biogenesis to compensate for the ETC impairment (Lee et al., 2000, Lee et al., 2003, Hansson et al., 2004). To address whether the defective OXPHOS system in WAH-1/AIF deficiency led to increased mtDNA copy number as a compensatory mechanism, I performed downregulation of *wah-1* in *C. elegans* mutants carrying different ETC defects. To this end, mutant strains were used, which carry loss-of-function mutations for the ETC genes *gas-1*, *mev-1* or *clk-1*. GAS-1 is one subunit of CI and loss of the *gas-1* gene leads to reduced CI activity and a shortened lifespan (Kayser et al., 2001). MEV-1 is the worm ortholog of the mammalian succinate dehydrogenase cytochrome b560 subunit of CII and *mev-1* loss-of-function leads to reduced CII activity and lifespan as well as increased ROS production (Ishii et al., 1998). CLK-1 is the ortholog of COQ7/CAT5, a highly conserved demethoxyubiquinone hydroxylase, necessary for the biosynthesis of ubiquinone (coenzyme Q), which shuttles electrons from CI or CII respectively, to CIII. Consequently, CI-CIII activity is inhibited in *clk-1* mutants, which results in increased lifespan (Kayser et al., 2004), decreased mitochondrial respiration and decreased ROS damage to mitochondrial proteins. Interestingly, mitochondria in *clk-1* mutants scavenge ROS more effectively than wildtype and show reduced oxidative stress (Yang et al., 2009). Therefore, *clk-1* mutants were used as a negative control as mtDNA copy number should not be elevated compared to wildtype animals.

As expected, *gas-1* and *mev-1* mutants showed a significant increase of mtDNA compared to the wildtype control (Figure 3-4), probably due to a compensatory increase of mitochondrial biogenesis caused by an impaired ETC. In contrast, the *clk-1* mutation did not lead to elevated mtDNA levels compared to N2 (Figure 3-4).

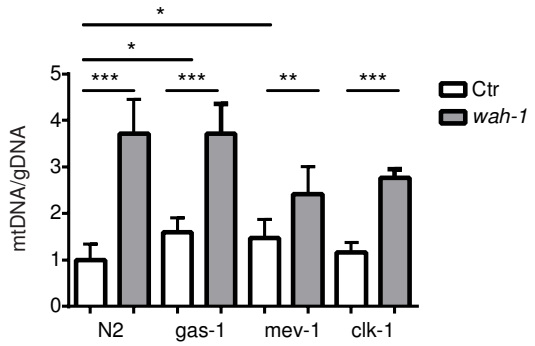


**Figure 3-4: Increase of mtDNA levels after knockdown of WAH-1/AIF is not induced by electron transport chain impairment. A** Relative mtDNA levels in N2, *mev-1(kn1)*, *gas-1(fc21)* and *clk-1(e2519)* animals at day 12 after *wah-1* (RNAi). Values represent fold difference relative to control conditions (n=3). Asterisks indicate statistical significance (unpaired Student´s *t*-test, *** $p < 0.001$).

However, reduction of WAH-1/AIF in these mutant backgrounds resulted in several-fold increase of mtDNA (Figure 3-4). This suggests that the ETC defect in WAH-1/AIF deficient background was not the primary cause of increased mtDNA.

*Increased mtDNA is not mediated by reactive oxygen species (ROS) or oxidative stress induced mitochondrial biogenesis*

Increased oxidative stress in patients suffering from mitochondrial disorders is associated with increased mitochondrial biogenesis and mtDNA replication (Lee et al., 2000). The effective coordination of gene expression, protein synthesis and transport during mitochondrial biogenesis is initiated by either anterograde signals send from the nucleus to the mitochondria or vice versa via retrograde signals that originate at the mitochondria (Whelan and Zuckerbraun, 2013). These signals include ROS, the AMP/ATP ratio, the mitochondrial unfolded protein response and oxidative stress (Whelan and Zuckerbraun, 2013). To address whether increased mitochondrial biogenesis contributes to increased mtDNA in WAH-1/AIF deficient conditions, I assessed signaling events and transcriptional regulators, which induce mitochondrial biogenesis as well as mitochondrial mass.

One important retrograde signal to induce mitochondrial biogenesis is ROS (Lee et al., 2000). To address whether increased ROS signaling led to increased mtDNA in WAH-1/AIF deficient conditions, I supplemented wildtype or *wah-1* RNAi-treated worms with vitamin C. Supplementation

of vitamin C, an antioxidant ROS scavenger, is a commonly used method to study ROS signaling in *C. elegans* (Yang and Hekimi, 2010).

Supplementation of vitamin C reduced mtDNA copy number in wildtype N2, probably due to decreased ROS signaling (Figure 3-5 A). However, supplementation with the antioxidant in animals with reduced WAH-1/AIF expression led to increased mtDNA copy number (Figure 3-5 A). This suggests that ROS were not mediating the increase in mtDNA upon WAH-1/AIF knockdown.

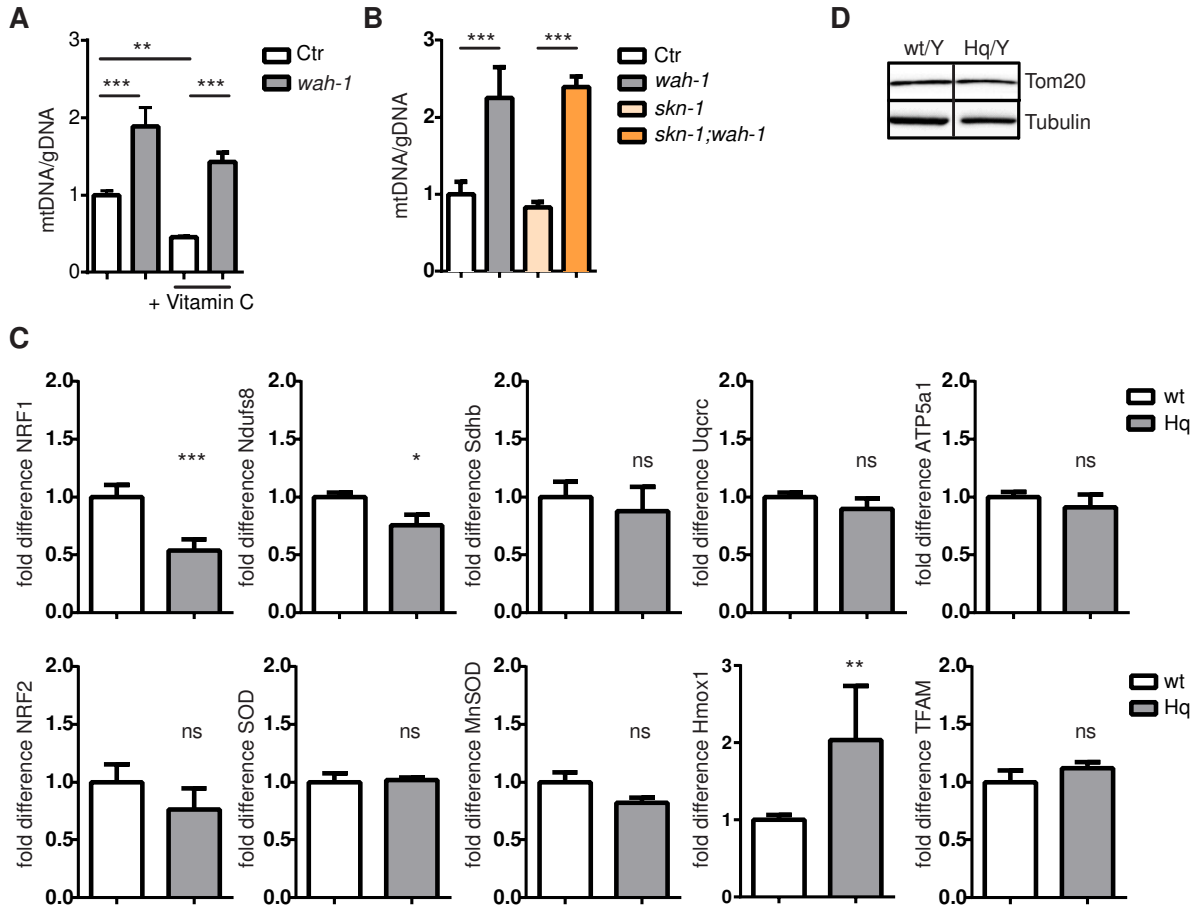


**Figure 3-5: Increased mtDNA in *WAH-1/AIF* deficient conditions is not a result of ROS signaling, increased oxidative stress, increased mitochondrial biogenesis or increased PGC1α activity. A** Relative mtDNA levels in N2 nematodes at day 12 after treatment with or without 0.5 mM vitamin C and knockdown of *wah-1* by RNAi. **B** Relative mtDNA content in N2 animals treated with *wah-1* (RNAi), *skn-1* (RNAi) and *wah-1;skn-1* (RNAi). **C** Immunoblot analysis of the translocase of the outer mitochondrial membrane (TOM20) in MEF cells derived from wildtype (wt/Y) or harlequin mice (Hq/Y). **D** Relative mRNA expression of NRF1 and its target genes NDUFS8 (CI), SDHb (CII), Uqcrc (CIII), ATP5a1 (CV) (upper row). Lower row shows mRNA expression of NRF2 and NRF2 target genes SOD2, MnSOD, Hmox1 and TFAM. qPCR was performed on 6 month old cerebella from wildtype control (wt) and harlequin mice (Hq). Values represent fold difference relative to control conditions. Asterisks show statistical significance (unpaired Student´s *t*-test, *** $p < 0.001$).

Next, I tested whether increased mitochondrial biogenesis caused by oxidative stress in general led to the observed mtDNA phenotype, by measuring mtDNA copy number in nematodes treated with *skn-1* RNAi. SKN-1 is a basic leucine zipper domain (bZip) transcription factor and the ortholog of the mammalian nuclear respiratory transcription factors (NRF), which regulates the adaptive oxidative stress response (Glover-Cutter et al., 2013). Downregulation of WAH-1/AIF in *skn-1* deficient nematodes resulted in increased mtDNA (Figure 3-5 B), suggesting that the response to oxidative stress did not mediate the effect of *wah-1* silencing on mtDNA copy number.

In mammals transcriptional regulation of mitochondrial biogenesis is mediated through the activity of peroxisome proliferator-activated receptor gamma coactivator-1 α (PGC1α). PGC1α activates and increases the expression of the nuclear respiratory transcription factors NRF1 and NRF2. These factors induce the transcription of genes essential for mitochondrial biogenesis, such as ETC components, mitochondrial structural proteins, mtDNA maintenance proteins and oxidative stress response proteins (Puigserver and Spiegelman, 2003).

By assessing the activity of PGC1α, I tested whether increased mitochondrial biogenesis contributed to increased mtDNA upon AIF reduction. To determine PGC1α activity, I measured NRF1 and NRF2 mRNA levels and the expression of their target genes in wildtype and harlequin mice cerebella (6 months of age). NRF1 target genes include ETC subunits such as Ndufsu8 (CI), Sdhb (CII), Uqcrc (CIII), ATP5a1 (CV) as well as TFAM, an essential protein for mtDNA replication and transcription. Transcriptional targets of NRF2 include antioxidative genes such as superoxide dismutase (SOD), manganese superoxide dismutase (MnSOD) and heme oxygenase (decycling) 1 (Hmox1). Interestingly, harlequin mice cerebella showed significantly reduced NRF1 mRNA levels (Figure 3-5 C). However, the expression of NRF1 target genes was unchanged compared to wildtype controls (Figure 3-5 C). Moreover, NRF2, SOD2 and MnSOD gene expression were unchanged but Hmox1 mRNA levels were significantly increased (Figure 3-5 C). Thus, there was no consistent increase of PGC1α targets NRF1/NRF2 and their target genes in harlequin mice compared to control littermates (Figure 3-5 C), suggesting that PGC1α activity was not induced in harlequin mice.

Finally, I assessed mitochondrial mass by western blot analysis of the mitochondrial structural protein TOM20 in harlequin and wildtype MEF cells. The western blot showed no difference between wildtype and harlequin cells, which indicates equal mitochondrial mass (Figure 3-5 D).

In conclusion, the increase of mtDNA in WAH-1/AIF deficient background was neither mediated by ROS signaling nor by an adaptive oxidative stress response in *C. elegans*. Moreover, loss of WAH-1/AIF did neither activate PGC1α induced mitochondrial biogenesis nor increased mitochondrial mass in harlequin mice.

## 3.3. Increase of mtDNA copy number in WAH-1/AIF deficiency is not mediated by common mtDNA synthesis pathways.

The mitochondrial genome encodes for 13 proteins, which are essential for OXPHOS system and mutations in mtDNA or genes involved in mtDNA maintenance processes have severe pathological consequences in humans (Taylor and Turnbull, 2005). Thus, proper mitochondrial metabolic function requires tightly controlled maintenance and replication of mtDNA.

Since AIF deficiency led to increased levels of mtDNA, I addressed whether this was due to increased mtDNA replication. Well-established mtDNA replication proteins in *C. elegans* are PAR-2.1, the ortholog of the mammalian mitochondrial single stranded binding protein (mtSSBP) (Sugimoto et al., 2008) and HMG-5, the ortholog of the mammalian mitochondrial DNA transcription factor A (TFAM) (Sumitani et al., 2011). MtSSBP and TFAM are considered two key components of the mtDNA replication machinery (Sugimoto et al., 2008, Sumitani et al., 2011).

First, I measured basal gene expression of *par-2.1* and *hmg-5* in wildtype and *wah-1* (RNAi)-treated nematodes. Notably, mRNA levels of both genes were not significantly increased in *wah-1* deficient animals (Figure 3-6 A).

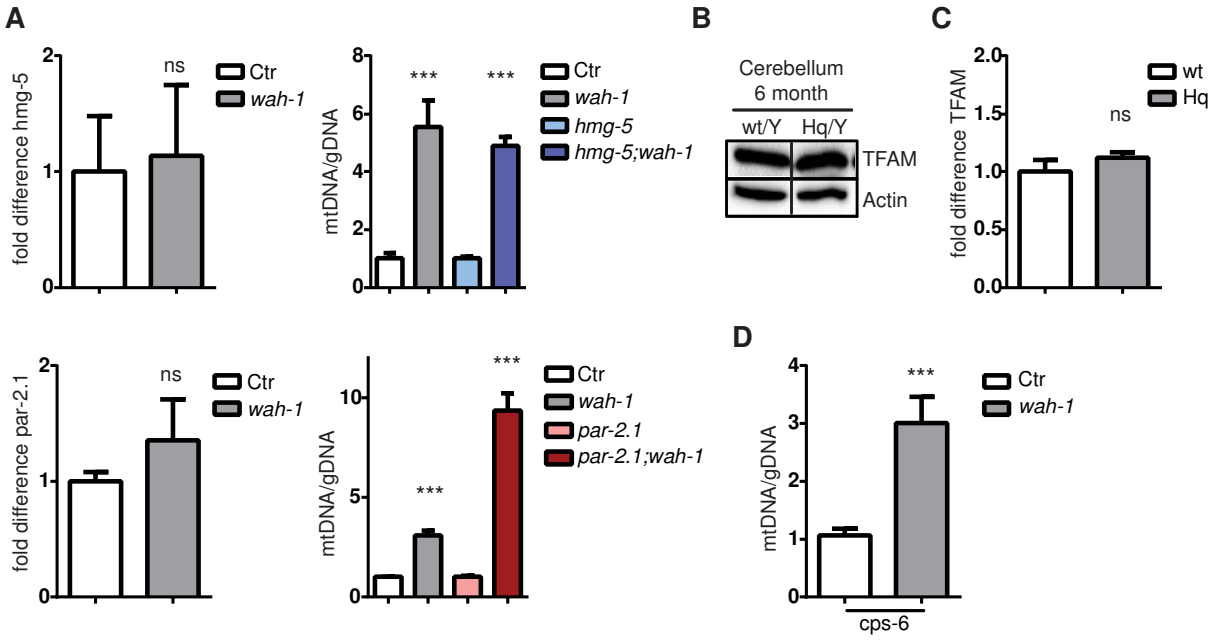


**Figure 3-6: Increase of mtDNA copy number upon WAH-1/AIF deficiency is independent of common mtDNA synthesis pathways. A** Relative mRNA levels of *hmg-5* and *par-2.1* in N2 animals after treatment with control or *wah-1* RNAi at day 4 (left). (right) Relative mtDNA in N2 animals subjected to *wah-1, hmg-5* and *hmg-5;wah-1* RNAi or *par-2.1* and *par-2.1;wah-1* RNAi, measured at day 12. **B** Western Blot analysis of TFAM in 6 month old harlequin and wildtype cerebella. **C** Relative mRNA expression of TFAM in 6 month old harlequin and wildtype cerebella. **D** Relative mtDNA copy number in *cps-6(ok1718)* animals after *wah-1 (RNAi* (W). Values represent fold difference relative to control conditions (n=3). Asterisks show statistical significance (unpaired Student´s *t*-test, *** $p < 0.001$).

Second, WAH-1/AIF was silenced in both *par-2.1* and *hmg-5* RNAi-treated worms and mtDNA copy number was determined. Interestingly, knockdown of neither mtSSBP/*par-2.1* nor TFAM/*hmg-5* abrogated the increase of mtDNA upon *wah-1* silencing (Figure 3-6 A). Third, I measured the amount of TFAM in cerebella of 6 month old wildtype and harlequin mice, which generally correlates with the amount of mtDNA. Notably, neither TFAM protein levels (Figure 3-6 B) nor gene expression (Figure 3-6 C) was increased in harlequin mice. These findings suggest that increased mtDNA replication was not causing increased mtDNA copy number in AIF deficiency.

Apart from TFAM and mtSSBP the mitochondrial endonuclease EndoG was proposed to be involved in mtDNA replication by providing primers required by DNA polymerase gamma to initiate replication of mtDNA (Cote and Ruiz-Carrillo, 1993). Moreover, the *C. elegans* EndoG ortholog CPS-6 was shown to directly interact with AIF (Wang et al., 2002). Thus, I tested whether this endonuclease was important for mtDNA increase after *wah-1*(RNAi). To this end, *cps-6* loss-of-function mutants

were subjected to *wah-1* RNAi and mtDNA copy number was detected. QPCR revealed that loss-of-function of *cps-6* did not abrogate the effect of *wah-1* silencing on mtDNA (Figure 3-6 D), suggesting that cps-6 was not involved in the increased mtDNA copy number upon WAH-1/AIF downregulation.

Finally, I investigated whether an altered or stalled mtDNA replication state induced a total increase of mtDNA. MtDNA replication occurs by a "strand-displacing"-model. Replication starts at the origin OH where it frequently terminates after approximately 700 bp downstream. This results in the 7S DNA, which forms a triple-stranded structure with the parental DNA, the displacement loop (D-loop). Thus, 7SDNA represents an intermediate of prematurely terminated replication and an increased ratio of 7S DNA to mtDNA points to a stalled replication cycle (Nicholls and Minczuk, 2014). However, measuring the 7S DNA and calculation of the 7S DNA to mtDNA ratio in cerebella derived from 6 month old wildtype and harlequin mice revealed no alterations of mtDNA replication (Figure 3-7) between the groups.

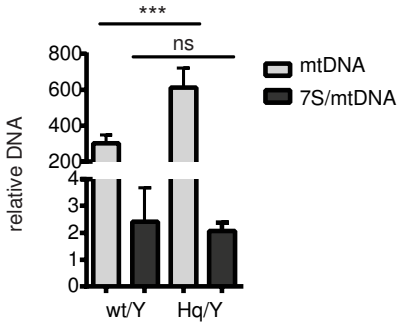


**Figure 3-7: Harlequin mice show a normal mtDNA replication cycle.** Relative mtDNA copy number and 7S DNA/mtDNA ratio in cerebella from 6 month old Harlequin mice (Hq/Y) and control littermates (wt/Y). Values represent fold difference relative to control conditions (n=3). Asterisks show statistical significance (unpaired Student´s *t*-test, *** $p < 0.001$).

In conclusion, the mtDNA replication proteins mtSSBP/*par-2.1*, TFAM/*hmg-5* and EndoG/*cps-6* were not involved in the increase of mtDNA upon AIF downregulation. Moreover, mtDNA replication was not altered in harlequin mice cerebella, suggesting that increased mtDNA copy number was a result of reduced mtDNA degradation rather than increased mtDNA replication.

## 3.4. Mitochondrial fusion and fission does not mediate changes in mtDNA upon WAH-1/AIF downregulation

Since increased mtDNA upon WAH-1/AIF knockdown was independent of several mtDNA replication proteins, impaired mtDNA degradation might lead to an accumulation of mtDNA. The mtDNA quality and copy number is maintained by different quality control systems, including mitochondrial fusion and fission processes (Chen et al., 2010, Ban-Ishihara et al., 2013). On the one hand, mitochondrial fusion represents an important mechanism to mix mitochondrial content and is therefore hypothesized to play an important role in functional complementation, especially of mutated or defective mtDNA (Nakada et al., 2009). In line with this, decreased mitochondrial fusion leads to mtDNA depletion and mitochondrial dysfunction (Chen et al., 2010). The fusion machinery requires the activity of OPA1 and Mitofusins (Song et al., 2009). On the other hand, mitochondrial fission is mainly catalyzed by DRP1 and represents an important mechanism for the degradation of dysfunctional mitochondria (Kageyama et al., 2014). Given the importance of fusion and fission to mtDNA quality control, I addressed whether these processes influenced mtDNA copy number after WAH-1/AIF downregulation. Therefore, I measured mtDNA copy number upon WAH-1/AIF knockdown in *C. elegans* strains with loss-of-function mutations for EAT-3/OPA1 and DRP-1 as wells as in animals with reduced FZO-1 (Mfn1) expression. Strikingly, neither loss of EAT-3/OPA1 or DRP-1 nor reduction of FZO-1/Mfn1 expression abrogated the increase of mtDNA upon WAH-1/AIF down regulation (Figure 3-8 A).

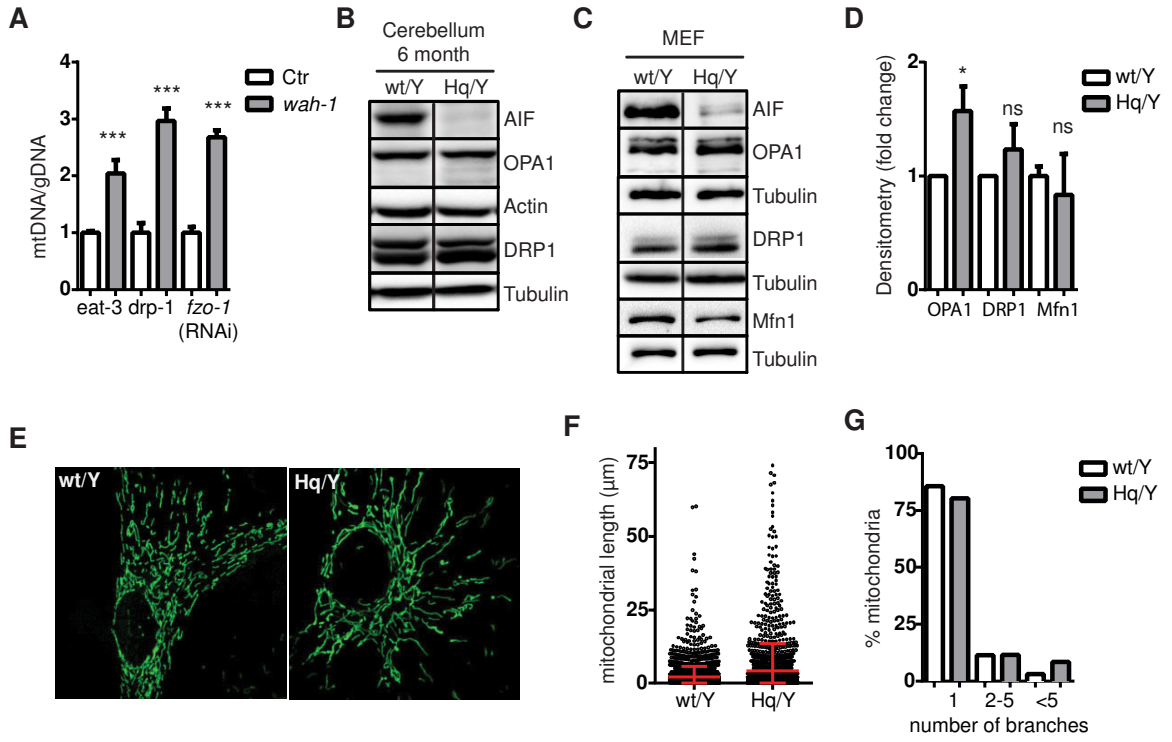


**Figure 3-8: Neither fusion nor fission processes mediate changes in mtDNA copy number after *WAH-1/AIF* knockdown. A** Relative mtDNA levels in N2, *eat-3(ad426);him(e1489)*, *drp-1(tm1108)* and *fzo-1*(RNAi) deficient animal at day 12 after *wah-1* (RNAi). **B** Immunoblot analysis and densitometry of fusion protein OPA1 and fission protein DRP1 in cerebella from 6 month old wildtype (wt/Y) and harlequin mice (Hq/Y). **C-D** Western Blot analysis and densitometry of OPA1, DRP1 and Mitofusin 1 (MFN1) in MEF cells derived from harlequin mice and control littermates. **E** Analysis and quantification of mitochondrial morphology by spinning disc microscopy in wildtype and harlequin MEF cells (experiment was performed with help of Fabio Bertan). **F-G** Quantification of mitochondrial length and number of mitochondrial branches in wildtype and harlequin MEF cells. Values represent fold difference relative to control conditions. Asterisks show statistical significance (unpaired Student´s *t*-test, *** $p < 0.001$).

Moreover, both OPA1 and DRP1 protein levels were similar in cerebella from 6 month old harlequin and wildtype mice (Figure 3-8 B). However, I observed increased OPA1 but not DRP1 or Mfn1 protein levels in MEF cells derived from harlequin mice in comparison to wildtype control cells (Figure 3-8 C-D).

Given the increase of OPA1 in MEF cells, we used spinning disk microscopy to visualize mitochondrial morphology. Interestingly, mitochondria of harlequin MEF cells showed increased fusion (Figure 3-8 E), mitochondrial length (Figure 3-8 F) and branching (Figure 3-8 G), which suggests a hyper-fused mitochondrial network in harlequin MEF cells.

Conclusively, loss of AIF led to increased mitochondrial fusion in harlequin fibroblast cells, however there was no detectable difference of fusion and fission proteins in harlequin mice cerebella compared to wildtype controls. This suggests that changes in mitochondrial morphology were tissue-specific and did not correlate with the increase of mtDNA observed after WAH-1/AIF downregulation in harlequin cerebella and MEF cells (data not shown). Moreover, neither fusion nor fission processes accounted for the increase of mtDNA copy number upon WAH-1/AIF deficiency in *C. elegans*.

## 3.5. Increase of mtDNA copy number is regulated by the cell cycle

The mitochondrial genome is constantly replicated in the mitochondrial matrix, independently from nuclear DNA replication (Fernandez-Silva et al., 2003). During progression through the cell cycle, the amount of both mitochondria and mtDNA is increased, to ensure passing enough mtDNA molecules to the daughter cell. Therefore, strong nuclear-mitochondrial communication is necessary to ensure successful cell proliferation and proper mitochondrial function in the daughter cell. In contrast to mtDNA the replication of the nuclear genome is strictly regulated and monitored by different checkpoints. The cell cycle comprises four different phases: A long growth phase (G1), DNA replication (S), followed by a short growth phase (G2) and finally cell division or mitosis (M). Whether mtDNA synthesis is coordinated with the cell cycle remains controversial. Replication might either occur continuously throughout the cell cycle (Falkenberg et al., 2007) or increases at specific phases such as S and G2 (Chatre and Ricchetti, 2013).

*Cell Cycle arrest abrogates increase of mtDNA after wah-1 downregulation*

Klein and colleagues reported cell cycle re-entry and subsequent induction of apoptosis in retinal granule cells in harlequin mice (Klein et al., 2002). MtDNA copy number is increased during the cell cycle, which raises the question whether cell cycle events accounted for the increase of mtDNA copy number in AIF deficient background.

To address whether the abundance of proliferative cells was important for mtDNA increase upon WAH-1/AIF downregulation, wildtype N2 nematodes were treated with the DNA replication inhibitor hydroxyurea (HU). HU inhibits the p53R subunit of the ribonucleotide reductase, leading to depletion

of the dNTP pool and resulting in cell cycle arrest of the proliferating germline (Brauchle et al., 2003). Since the germline contains the only cycling cells present in *C. elegans*, animals incubated with HU become sterile (Brauchle et al., 2003). Strikingly, incubation with HU completely abrogated the increase of mtDNA in wildtype nematodes after WAH-1/AIF knock down (Figure 3-9 A).

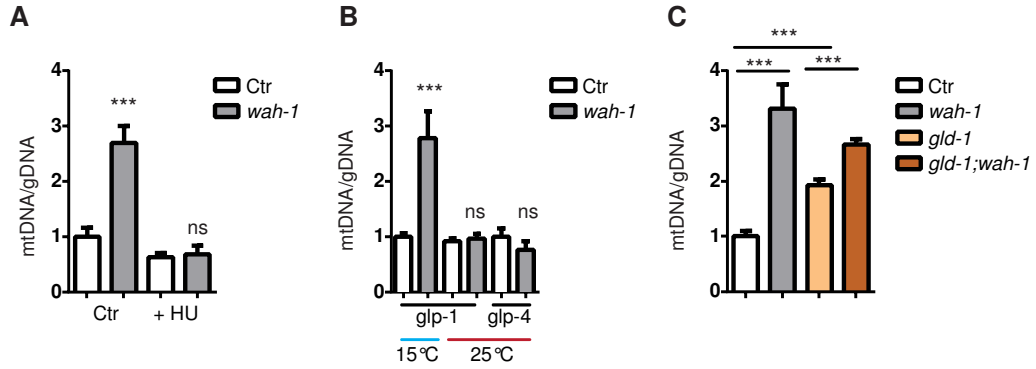


**Figure 3-9: Increase of mtDNA in WAH-1/AIF deficient background is mediated by the proliferating germline. A** Relative mtDNA in N2 either treated with 25mM hydroxyurea (HU) after *wah-1* RNAi (W) relative to control RNAi (with untreated worms used as control). Relative mtDNA levels in *glp-1(e2141)* and *glp-4(bn2)* animals at day 12 after treatment with control (Ctr) or *wah-1* RNAi. Animals were grown at the permissive temperature 15°C or transferred to nonpermissive temperature of (25°C) at L1/L2 larvae stage. Relative mtDNA copy number in N2 animals grown on *wah-1* (RNAi), *gld-1* (RNAi) or *wah-1;gld-1* (RNAi).

To confirm whether the lack of mitotic cell division in the germline abrogates the increase of mtDNA upon WAH-1/AIF knockdown, I genetically removed the proliferating germline using *glp-1(e2141)* or *glp-4(bn2)* homozygous mutants. Loss of function of *glp-1* or *glp-4* leads to the complete absence of proliferating cells resulting in sterile animals. Nematode strains containing a temperature sensitive allele for *glp-1(e2141)* or *glp-4(bn2)* were subjected to *wah-1* RNAi knockdown and mtDNA content was measured. Notably, while these nematode strains show a wildtype phenotype when maintained at 15°C (permissive temperature), the mutant alleles become active when worms are shifted to 25°C (nonpermissive temperature). Strikingly, the effect of *wah-1* silencing on mtDNA copy number was completely abolished in *glp-1* and *glp-4* mutants grown at the nonpermissive temperature (25°C), indicating that mitotic cell division in the *C. elegans* germline was necessary for the increase of mtDNA upon *wah-1* silencing (Figure 3-9 B). Finally, I addressed whether excessive germline proliferation might reverse this effect. Therefore, I measured mtDNA copy number in animals grown on *gld-1;wah-1*(RNAi). GLD-1 is a key regulator of stem cell differentiation in the germline and knockdown of *gld-1* leads to overproliferation of mitotic cells, which subsequently results in a gonadal tumor (Kadyk and

Kimble, 1998). As expected mtDNA copy number was higher in animals grown on *gld-1*(RNAi) compared to the control but the double knockdown of *gld-1* and *wah-1* led to a further increase of mtDNA (Figure 3-9 C).

In conclusion, ablation of proliferating cells in *C. elegans* completely abrogated the increase of mtDNA upon WAH-1/AIF knockdown. However when germ cells were unable to undergo differentiation WAH-1/AIF deficiency led to increased mtDNA copy number. This suggested that the switch between proliferation and cell differentiation and therefore a specific cell cycle phase was mediating the effect of *wah-1* silencing on mtDNA copy number.

*Cyclin E/cye-1 mediates increase of mtDNA copy number*

To determine which components of the cell cycle signaling pathway mediated the increase of mtDNA upon WAH-1/AIF reduction, several *C. elegans* strains containing mutations in cell cycle relevant genes were subjected to *wah-1* RNAi. MtDNA copy number after *wah-1* silencing was measured in *cdk-5*, *cdc-25*, *chk-2*, *mre-11* and *cye-1* homozygous mutants. CDK-5 is the homolog of mammalian cyclin dependent kinase 5 (Cdk-5), which is not strictly a cell cycle dependent cyclin but rather is important for neuronal development (Juo et al., 2007). Thus, this strain was used as a negative control. The phosphatase CDC-25 mediates the activation of different cyclin dependent kinases, such as cyclin A and cyclin B, during cell cycle progression (Ashcroft et al., 1999). CHK-2 is the ortholog of mammalian Chk2 and an important protein kinase during cell cycle checkpoints since its activation by DNA damage leads to cell cycle arrest (Higashitani et al., 2000). MRE-11 acts in parallel to CHK-2 and its activation by DNA damage during cell cycle checkpoints can result in cell cycle arrest (Chin and Villeneuve, 2001). The ortholog of mammalian Cyclin E, CYE-1 is required for cell cycle progression from G1 to S phase by forming a complex with the cyclin dependent kinase CDK-2 (Kipreos, 2005).

Neither loss of function of *cdk-5*, *cdc-25*, *chk-2* nor *mre-11* abrogated the effect of *wah-1* silencing on mtDNA copy number (Figure 3-10 A). However, *cye-1* loss-of-function mutants did not show any mtDNA increase after *wah-1* knockdown (Figure 3-10 A).

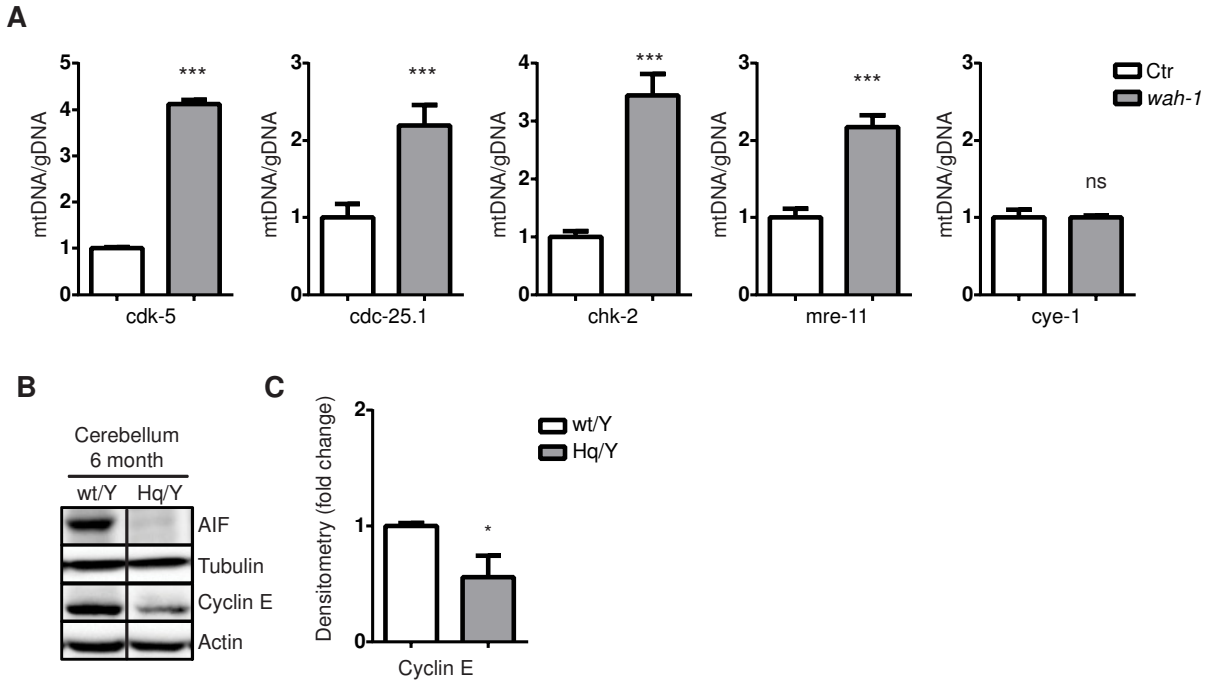


**Figure 3-10: Increase of mtDNA in *WAH-1/AIF* deficient background is mediated by *cye-1*/CyclinE**

**A** qPCR analysis of mtDNA copy number in *cdk-5(ok626)*, *cdc-25.1(nr2036/dpy-5(e61)unc-13(e450))*, *chk-2(gk212), mre-11(ok179)* and *cye-1(ar95a)* after treatment with control (C) and *wah-1* RNAi. **B-C** Immunoblot and densitometry analysis of AIF and Cyclin E in 6 month old cerebella from harlequin mice (Hq/Y) and control (wt/Y) littermates. Values represent fold difference relative to control conditions. Asterisks show statistical significance (unpaired Student´s *t*-test, *** $p < 0.001$).

Furthermore, cyclin E protein levels in cerebella from 6 month old harlequin mice were significantly reduced compared to wildtype littermates (Figure 3-10 B-C), suggesting that cycline E was an important factor in mediating the increase of mtDNA in WAH-1/AIF deficient conditions.

*Loss of AIF does not alter cell cycle progression in harlequin fibroblast cells*

Lowered cyclin E protein levels could account for cell cycle alterations during G1-S transition in harlequin mice cerebella. To assess whether loss of AIF leads to altered cell cycle progression, I performed a cell cycle analysis to determine the percentage of cells in G1, S, G2 or mitosis phase. To this end, nDNA in MEF cells derived from wildtype and harlequin mice were stained with propidium iodid. Then the cells were subjected to cell cycle analysis by flow cytometry. Interestingly, there was no

detectable difference between control and harlequin derived cell populations. In both cases around 75% of the cells are present in the G1-phase, around 5% in G1/S and about 20% in G2 (Figure 3-11 A).

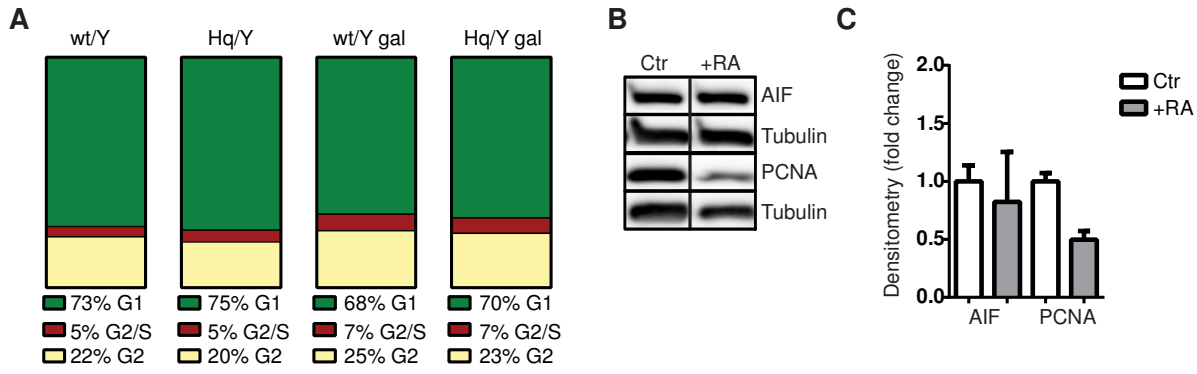


**Figure 3-11: Loss of AIF does not alter cell cycle progression in harlequin MEF cells and AIF protein levels do not change during G1/G0 transition. A** Flowcytometric cell cycle analysis after propidium iodid staining of MEF cells derived from harlequin mice (Hq/Y) and control (wt/Y) littermates. **B-C** Immunoblot and densitometry analysis of AIF and the proliferation marker PCNA in SH-SY5Y cells after differentiation induced by supplementation with 10 µM retinoic acid (RA).

Cells with impaired OXPHOS, such as harlequin MEF cells, are highly glycolytic, therefore it is difficult to study cellular effects caused by mitochondrial dysfunction. Thus, exchanging glucose for galactose in the cell culture medium forces cells to rely on aerobic metabolism and uncovers the impact of OXPHOS impairment on cellular processes (Aguer et al., 2011). However, the fractions of wildtype and harlequin MEF cells in different phases of the cell cycle were similar between glucose and galactose culturing conditions (Figure 3-11 A), suggesting that ETC impairments in harlequin MEFs did not effect cell cycle progression. Moreover, to address whether cells that leave the cell cycle and differentiate display changes in AIF protein levels, I performed an alternative experiment by differentiating SH-SY5Y cells and determining AIF protein levels. SH-SY5Y cells represent an established *in vitro* model to study neuronal function and differentiation (Agholme et al., 2010). Under standard culturing conditions SH-SY5Y cells are constantly proliferating but supplementation of retinoic acid induces their differentiation (Agholme et al., 2010). Differentiated and cycling SH-SY5Y cells were harvested and western blot analysis were performed using AIF and PCNA antibodies. PCNA is a protein, which is expressed in proliferating cells. Accordingly, PCNA protein levels decreased when cells underwent differentiation (Figure 3-11 B-C). However, AIF protein levels were similar in both proliferating and differentiated conditions (Figure 3-11 B-C). In summary, AIF deficicency in

MEF cells did not alter cell cycle progression and AIF protein levels did not change upon differentiation of SH-SY5Y cells.

## 3.6. Increase of mtDNA in WAH-1/AIF deficient conditions is mediated by the DNA Damage Checkpoint protein atl-1/ATR

Since accurate maintenance of genomic integrity is crucial for cell survival, both replication and quality of nDNA are monitored by different DNA damage checkpoints during cell cycle progression (Harper and Elledge, 2007). All DNA damage responses, including double strand breaks, replication stress and nucleotide damage are orchestrated by the two main DNA damage checkpoint kinases Ataxia telangiectasia mutated (ATM) and Ataxia- and Rad-related (ATR) (Harper and Elledge, 2007). Activation of these kinases leads to a comprehensive activation of downstream pathways, which induce cell cycle arrest at the G1/S, S, or G2/M checkpoint and subsequently initiate DNA repair or apoptosis, denpending on the severity of the damage (Harper and Elledge, 2007).

As described above, the increase of mtDNA copy number after downregulation of WAH-1/AIF was associated with alteration of signaling factors during cell cycle progression. Thus, specific signaling cascades in G1 or during G1/S transition might be involved, given that CYE-1/Cyclin E was associated with the mtDNA increase after WAH-1/AIF knockdown. Therefore, I addressed whether the DNA damage checkpoint proteins ATM/ATR were important for the increase of mtDNA after WAH-1/AIF downregulation. To this end, I used *C. elegans* strains harboring mutations in the *atl-1*/ATR, *atm-1*/ATM and *cep-1*/p53 genes. The mammalian tumor supressor p53/*cep-1* is an important downstream target of ATM and was additionaly implicated in the regulation of mtDNA (Achanta et al., 2005, Saleem and Hood, 2013).

Interestingly, neither loss of function of *atm-1* and *cep-1* nor overexpression of *cep-1*/p53 abrogated the increase of mtDNA upon *wah-1* (RNAi) treatment. However, worms harboring a loss-of-function mutation for *atl-1*/ATR showed no increase of mtDNA (Figure 3-12 A), suggesting that *atl-1*/ATR and DNA damage signaling was important for the increase of mtDNA in WAH-1/AIF deficiency.

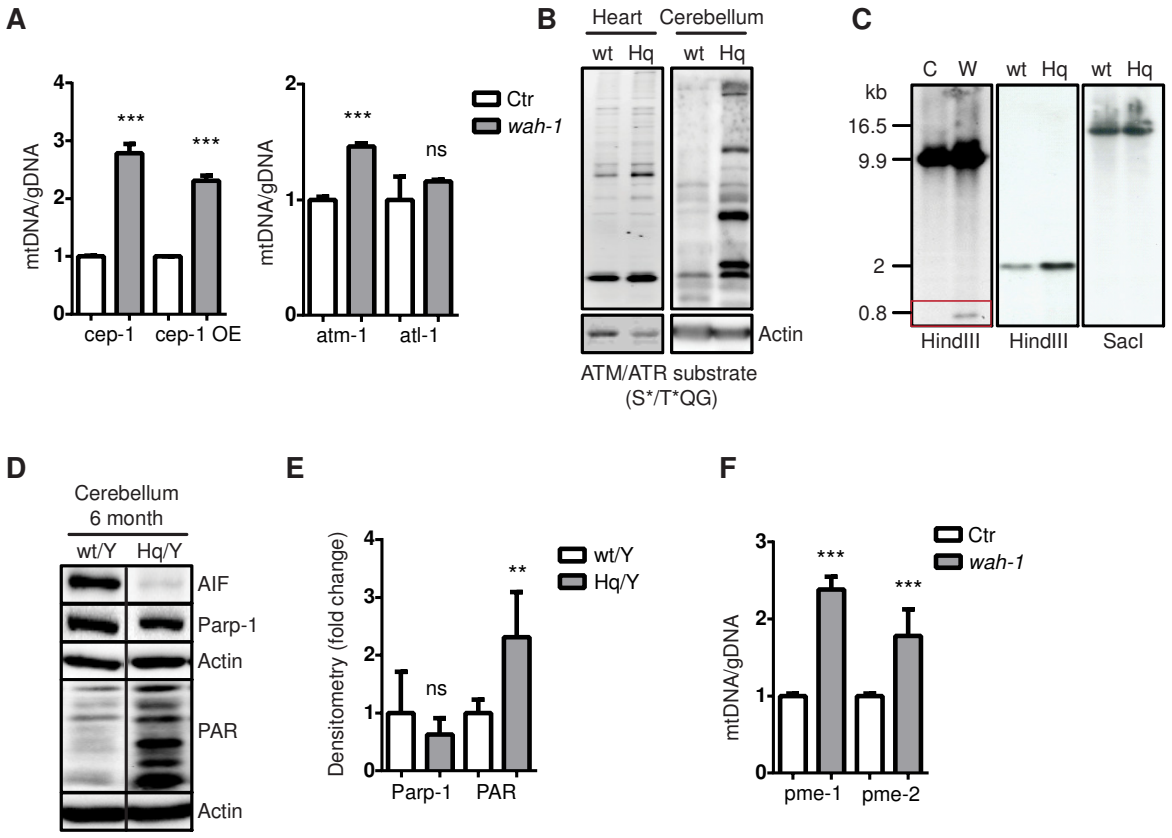


**Figure 3-12: Increased mtDNA copy number after knockdown of *WAH-1/AIF* is mediated by the DNA damage checkpoint protein Atl-1 and loss of AIF induces activity of Parp proteins. A** Relative mtDNA copy number in *atm-1(gk186)*, *atl-1(tm853)/nT1*, *cep-1(gk138)* and cep-1 overexpressing animals at day 12 after *wah-1* RNAi. **B** Immunoblot analysis of the ATM/ATR substate (S*/T*QG) phospho-Ser/phospho-Thr followed by Gln and Gly residues in heart and cerebella from 6 month old harlequin mice (Hq) and control (C) littermates. **C** Southern blot analysis of mtDNA from wildtype N2 after treatment with *wah-1* (RNAi) (W) and 6 month old cerebella from harlequin mice (Hq) and control (wt) littermates. Digestion with the restriction enzyme HindIII results in a 9.9 kb fragment in C. elegans and a 2 kb fragment in mice if mtDNA is not altered, while incubation with SacI results in linearized mtDNA (16.5 kb) in mice. **D-E** Immunoblot and densitometry analysis of AIF, Parp-1 and Poly(ADP-ribose) (PAR) in 6 month old cerebella derived from wildtype controls (wt/Y) and harlequin mice (Hq/Y). **F** Relative mtDNA copy number in *pme-1(ok988)* and *pme-2(ok344)* animals after *wah-1* (RNAi) treatment. Values represent fold difference relative to control conditions. Asterisks show statistical significance (unpaired Student´s *t*-test, *** $p < 0.001$).

In addition, total activity of ATM/ATR was determined by performing a western blot analysis using an ATM/ATR substrate antibody in heart and cerebellum of 6 month old wildtype and harlequin mice. The ATM/ATR antibody detects phosphorylated serine and threonin in the S*/T*QG motif, which is exclusivley phosphorylated by ATM and ATR. Strikingly, both tissues showed increased phosphorylated ATM/ATR motifs, indicating a strong activation of the two kinases (Figure 3-12 B).

Since, nDNA damage was not reported in harlequin mice, I addressed whether mtDNA was damaged by performing a southern blot analysis in nematodes and mice in a WAH-1/AIF deficient background. To this end, mtDNA extracted from nematodes treated with *wah-1*(RNAi) and 6 month old harlequin mice cerebella were digested with restriction enzymes and mtDNA fragments were detected with a mtDNA-specific probe. In this assay full-length mtDNA in nematodes yielded a 9.9 kb fragment, while in mice either 2 kb or 16.5 kb long fragments. The southern blot revealed alterations of mtDNA quality in nematodes after *wah-1* RNAi treatment, as shown by the 0.8 kb fragment. However, this finding was not reproducible in harlequin mice given that mtDNA derived from harlequin cerebella showed similar fragments compared to littermate controls (Figure 3-12 C).

A different method to determine general DNA damage is to measure Poly(ADP-ribose) polymerase (PARP) protein activity. PARP proteins are involved in a variaty of cellular processes but their classical role is to assist in DNA damage repair pathways, with Parp1 being the best characterised protein family member (Burkle and Virag, 2013). Therefore, I measured Parp-1 protein levels in cerebella from 6 month old harlequin mice. The western blot analysis revealed no difference in Parp1 protein levels between wildtype and harlequin mice cerebella (Figure 3-12 D-E). Thus, I determined the level of poly(ADP-ribosyl)ation (PARylation), a posttranscriptional modification catalysed by PARP enzymes. PAR polymer acceptors include histones and other DNA-associated proteins, thereby regulating chromatin organisation, DNA repair and DNA replication (Burkle and Virag, 2013).

Remarkably, cerebellar tissue of harlequin mice showed significantly increased levels of PAR polymers (Figure 3-12 D-E), suggesting increased activity of Parp enzymes. To address, whether increased PARylation resulted in increased mtDNA upon WAH-1/AIF deficiency, I silenced *wah-1* in *C. elegans* strains with loss of function mutations for the mammalian orthologs of Parp1 and Parp2, *pme-1* and *pme-2*. Neither *pme-1* and *pme-2* abrogated the increase of mtDNA after *wah-1* silencing, indicating that parylation events were not mediating the changes in mtDNA copy number (Figure 3-12 F).

In conclusion, the increase of mtDNA was mediated by the DNA damage checkpoint protein *atl-1*/ATR in *C.elegans*. Additionally, the DNA damage response proteins ATM/ATR kinases and PARP showed increased activity in the cerebellum of 6 month old harlequin mice compared to littermate controls.

# 4. Discussion

Mitochondria are crucial for cellular functions and mitochondrial impairments not only contribute to the ageing process but cause an array of human pathologies, such as neurodegenerative diseases, mitochondrial disorders, diabetes and cancer.

Mitochondrial dysfunction is caused by alterations of proteins important for mitochondrial maintenance or the OXPHOS system. Genetic mutations causing such alterations can either be present on nuclear or mitochondrial genes. However, mtDNA mutations or impairments of its maintenance proteins are the primary cause of mitochondrial disorders (Taylor and Turnbull, 2005, Schapira, 2012). Consequently, increasing our knowledge of mtDNA regulation and maintenance is essential for the development of treatments for mitochondrial dysfunction and its devastating effects on human health.

In this context, AIF plays a Janus-like role. It is a pro-death factor but is also indispensable for mitochondrial function, as AIF dysfunction leads to severe mitochondrial encephalomyopathy in humans (Ghezzi et al., 2010). Patients carrying the AIF-R201 mutation showed a depletion of mtDNA, suggesting that AIF is implicated in mtDNA maintenance (Ghezzi et al., 2010).

With the present study I aimed to elucidate the involvement of AIF in the regulation of mtDNA copy number by using *C. elegans* and harlequin mice as model systems.

My data demonstrate for the first time the involvement of AIF in regulating mtDNA. This regulation was highly evolutionary conserved from the nematode *C. elegans* to mice and occurs independently of previously described mechanisms.

Reduced expression levels of AIF led to a several-fold increase of mtDNA in *C. elegans* treated with *wah-1* RNAi and in harlequin mice, which show reduced AIF protein levels. Increased mtDNA copy number did not result in altered expression of mitochondrial genes, even though protein levels of CI and CIV were changed in harlequin mice cerebella. This suggests that AIF regulates the ETC composition on a post-transcriptional level. These findings are in line with studies on AIF deficient ES-cells, which showed no altered transcription of nuclear-encoded ETC genes despite their ETC defects (Vahsen et al., 2004). Although AIF interacts with RNA *in vitro* (Vahsen et al., 2006), there was no detectable alteration of mtRNA expression and therefore it is unlikely that AIF interacts with mtRNA *in vivo*. Moreover, stable mtRNA translation suggests that additional mtDNA molecules are

not utilized to enhance transcription of ETC genes to compensate for impaired respiratory complex composition. Therefore, how does AIF deficiency induce increased mtDNA copy number?

This study addressed several possibilities that might explain the increase of mtDNA following AIF knockdown (See figure 4-1). These possibilities include increased mtDNA copy number as an indirect consequence of AIF deficiency, by either increased mtDNA replication or decreased mtDNA degradation. Furthermore, AIF might also directly interact with mtDNA by either stalling replication or assisting in mtDNA degradation (See figure 4-1).

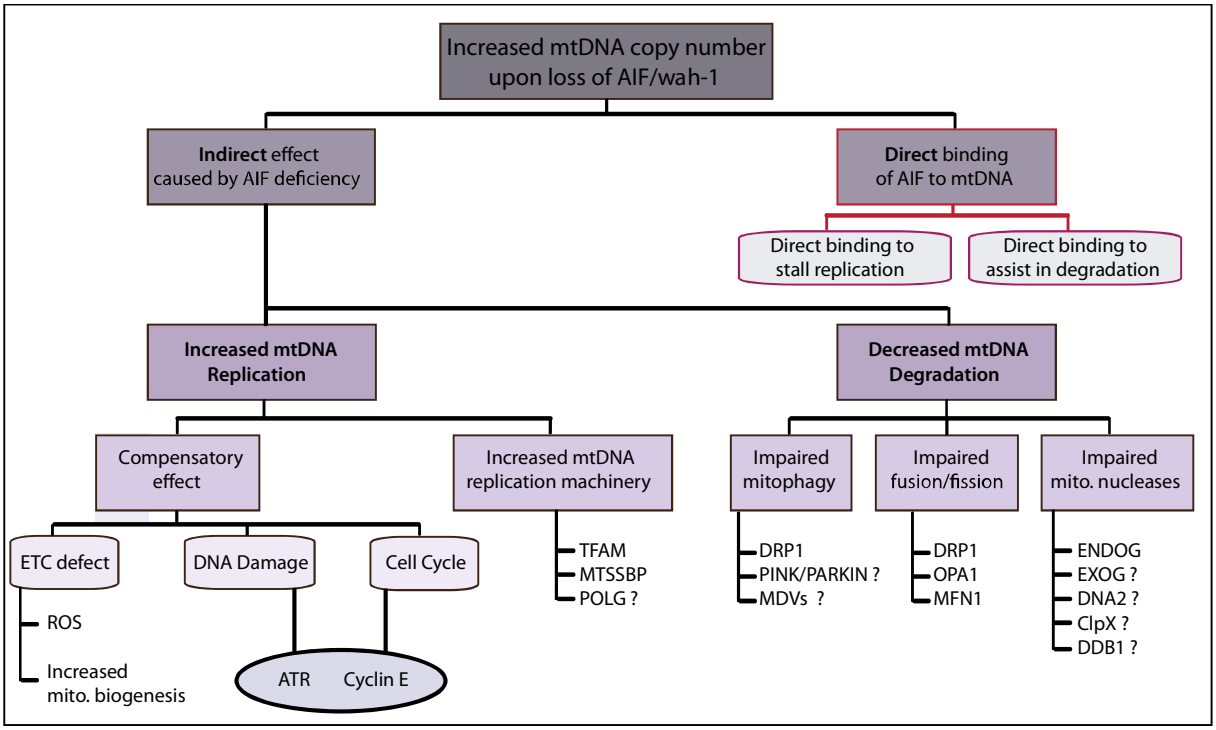


**4-1: Overview of effects that might lead to increased mtDNA copy number upon WAH-1/AIF deficiency.**

AIF represents an important protein for functional mitochondrial respiration and morphology and reduction of AIF leads to ETC impairments (Sevrioukova, 2011). Thus, cellular compensatory programs that increase mitochondrial mass to overcome impairments of the ETC might increase mtDNA replication. A well-established compensatory mechanism to deal with mitochondrial dysfunction is PGC1α induced mitochondrial biogenesis, including increased mtDNA replication (Lee et al., 2000). However, reduction of WAH-1/AIF in nematodes harboring a severe ETC defect, such as *gas-1*, *mev-1* of *clk-1* homozygous mutants, led to increased mtDNA copy number. In this context, neither ROS signaling nor increased mitochondrial biogenesis driven by PGC1α could be attributed to

the effect of WAH-1/AIF reduction on mtDNA. Strikingly, AIF deficiency did not induce a compensatory increase of mitochondrial biogenesis in mice although AIF deficiency leads to mitochondrial dysfunction.

Increased mtDNA replication could also be attributed to the upregulation of key mtDNA replication proteins. However, there was no detectable increase of TFAM in harlequin mice and downregulation of the essential mtDNA replication proteins *par-2.1* and *hmg-5* had no effect on mtDNA after downregulation of *wah-1* in nematodes. These observations point to decreased mtDNA degradation rather than increased replication.

The mitochondrial genome is redundant, with thousands of copies per cell. Therefore, a substantial fraction of mtDNA can be degraded without detrimental consequences since its loss is compensated by constant replication processes. This mtDNA turnover was already described 45 years ago (Gross et al., 1969). However, the molecular mechanisms that facilitate mtDNA degradation are still not well defined, even though many studies have reported mtDNA degradation upon oxidative stress. For instance, treatment of MEF cells with hydrogen peroxide resulted in mtDNA damage and loss of mtDNA (Furda et al., 2012) and incubation with lipopolysaccharide, an inducer of *in vivo* oxidative stress, induced mtDNA depletion in rat liver (Suliman et al., 2003). Currently, the only reported and defined process that degrades mtDNA is mitophagy. Mitophagy is the selective degradation of damaged mitochondria by autophagy. In this process, PTEN-induced putative kinase protein 1 (PINK1) recruits the cytosolic E3 ubiquitin ligase Parkin to damaged mitochondria (Narendra et al., 2008). This leads to the enclosure of whole mitochondria by autophagosomes that fuse with lysosomes for mitochondrial degradation. Mitophagy depends on the fission protein Drp1, which generates small mitochondria that can be engulfed by autophagosomes (Twig et al., 2008, Kageyama et al., 2012). However, it is unlikely that defective mitophagy led to increased mtDNA in WAH-1/AIF deficient conditions since nematodes defective for fusion or fission processes, such as EAT-3/OPA1 and DRP-1 mutants, display increased mtDNA upon *wah-1* reduction.

More recently, an alternative mitochondrial quality control mechanism facilitated by mitochondrial derived vesicles (MDVs) was discovered (Neuspiel et al., 2008, Braschi et al., 2010, Soubannier et al., 2012a). MDVs are generated by incorporation of protein cargos from all mitochondrial compartments and are either targeted to peroxisomes (Neuspiel et al., 2008, Braschi et al., 2010) or to lysosomes for degradation (Soubannier et al., 2012a). MDVs that are targeted to lysosomes for degradation are

selectively enriched with oxidized proteins and this process is stimulated by oxidative stress (Soubannier et al., 2012b). The formation of MDVs requires PINK1 and Parkin but occurs independently of Drp1 (Soubannier et al., 2012a). Therefore, it might be interesting to address whether this mechanism is altered in AIF deficient conditions by either assessing PINK1/Parkin accumulation in mitochondria or quantification of MDVs in cells or brain tissue derived from harlequin mice.

Degradation of mtDNA by mitochondrial nucleases has not been reported, yet. Currently, only six mitochondrial nucleases have been identified and all are part of the mtDNA repair machinery. For instance, mitochondrial genome maintenance exonuclease 1 (MGME1) is a mitochondrial exonuclease that processes mtDNA during replication (Szczesny et al., 2013) and loss of MGME1 leads to accumulation of 7S DNA due to incomplete processing of mtDNA 5'ends (Nicholls et al., 2014). Only one recent study linked mtDNA degradation with mitochondrial nucleases, in the context of viral infection. Herpes simplex virus 1 (HSV-1) infection leads to a rapid decrease of mtDNA mediated by the activity of the mitochondrial nucleases EndoG and endonuclease G-like 1 (ExoG) (Duguay and Smiley, 2013). EndoG was proposed to be involved in mtDNA replication and copy number control (Ohsato et al., 2002, McDermott-Roe et al., 2011) and directly binds to AIF during apoptosis (Wang et al., 2002). However, loss of function of the EndoG ortholog *cps-6* in *C. elegans* did not abrogate the effect on mtDNA copy number in WAH-1/AIF deficient conditions. Therefore, ExoG represents a good candidate that might be involved in regulation of mtDNA in AIF deficient conditions.

Since AIF binds to nucleases such as EndoG and CypA during apoptosis to become an active DNAase, one can hypothesize that AIF binds to such nucleases in mitochondria to form a "mtDNA degradasome", to actively participate in mtDNA degradation. Interestingly, AIF neither binds nor condenses relaxed, circular DNA, although it can interact with negatively supercoiled DNA and preferentially binds lineralized DNA (Vahsen et al., 2006). Furthermore, when AIF is combined with hybrid DNA molecules, which contain a single-stranded as well as a double stranded moiety, it preferentially binds to single-stranded DNA and causes spreading of such molecules, similar to classical single stranded proteins such as replication protein A (Vahsen et al., 2006). This is very interesting given that mtDNA can be negatively supercoiled and exists as a double-stranded and single-stranded DNA hybrid molecule owing to the D-loop structure (Pohjoismaki and Goffart, 2011). In this context, ExoG possesses nicking activity towards supercoiled DNA, which results in single stranded fractions of DNA (Cymerman et al., 2008). A combined interaction with AIF and ExoG

represents an interesting model for mtDNA degradation. AIF might serve as a scaffold that allows ExoG to degrade mtDNA molecules and at the same time, since AIF preferentially binds lineralized DNA, clusters mtDNA fragments for downstream degradation.

The effect of WAH-1/AIF deficiency on mtDNA copy number was completely abrogated in nematodes lacking the proliferative germline, such as *glp-1* and *glp-4*. In addition, worms lacking the protein Cyclin E/CYE-1 did not show increased mtDNA after WAH-1/AIF knockdown. Furthermore, WAH-1/AIF deficiency in nematodes with reduced GLD-1 expression, which disables cells to undergo differentiation, led to increased mtDNA copy number. These findings suggest that the block of proliferating cells per se was not mediating the increase of mtDNA after WAH-1/AIF knockdown. Thus, it is likely that signaling processes during specific cell cycle phases such as the switch between proliferation and cell differentiation led to increased mtDNA copy number.

In addition, cyclin E protein levels were reduced in harlequin mice cerebella. However, harlequin MEF cells did not show any impairment in cell cycle progression. Therefore, cyclin E might be an important signaling molecule leading to increased mtDNA. Increased expression of cyclin E during G1-phase drives cell entry into S-phase (Sherr, 1994). However, ubiquitous knockout of cyclin E in mice showed that it is largely dispensable for mouse development (Geng et al., 2003). Albeit its role in cell cycle regulation cyclin E is involved in neuronal function. cyclin E expression is not only restricted to proliferating cells, it is highly expressed in postmitotic neurons in the adult brain but not in astrocytes (Odajima et al., 2011). Interestingly, in differentiated neurons cyclin E forms a complex with the cyclin dependent kinase 5 (Cdk5) and disruption of this complex leads to Cdk5 overactivation (Odajima et al., 2011). Cdk5 is a Cdk-related protein that regulates neuronal differentiation, synaptic plasticity as well as memory formation (Lopes and Agostinho, 2011) and overactivation of Cdk5 is associated with several neurodegenerative disorders such as Alzheimer´s disease (Lopes et al., 2010), amyotrophic lateral sclerosis (Nguyen et al., 2001) and Parkinson´s disease (Alvira et al., 2008). Furthermore, Cdk5 dysregulation is involved in cell cycle re-entry in several neurodegenerative conditions, which leads to apoptosis and neuronal demise (Hoglinger et al., 2007, Lopes et al., 2009, Zhang et al., 2010). Harlequin mice show reduced cyclin E protein levels in the cerebellum, which might lead to the disruption of the cyclin E/Cdk5 complex and a subsequent overactivation of Cdk5. This dysregulation of Cdk5 might lead to cell cycle re-entry of postmitotic neurons as observed in harlequin mice (Klein et al., 2002). This hypothesis might be addressed by assessing Cdk5 localisation,

since its toxic effects are associated with the translocation either from the synaptic compartment to the cell body or from the nucleus to the cytosol (Zhang et al., 2008, Lopes et al., 2010).

During cell cycle progression the quality of DNA is monitored at different checkpoints by the DNA damage checkpoint proteins ATM and ATR (Harper and Elledge, 2007). Interestingly, defective DNA damage checkpoint protein ATL-1/ATR but not ATM-1/ATM abrogated the effect of WAH-1/AIF downregulation on increased mtDNA copy number in nematodes. Moreover, the activity of ATM/ATR as well as Parp proteins was highly increased in harlequin mice cerebella, suggesting an increased DNA damage response. Inactivation of *atl-1*/ATR in nematodes results in a mild oxidative stress response and a significant reduction of mtDNA independently of ribonucleotide reductases (Mori et al., 2008, Suetomi et al., 2013). Therefore, at least in *C. elegans* ATL-1/ATR is involved in mtDNA and mitochondrial maintenance (Mori et al., 2008). Given that the mitochondrial genome undergoes increased replication prior to cell division (Chatre and Ricchetti, 2013), it is possible that the coordination of increased mtDNA replication with the cell cycle is mediated by ATL-1/ATR. Under physiological conditions ATL-1/ATR might regulate the activity of mtDNA replication proteins by phosphorylation, leading to increased mtDNA replication during specific cell cycle phases (Figure 4-2 A).

Assuming that AIF is involved in mtDNA degradation the resulting mtDNA copy number in the daughter cells as well as the mtDNA repair response should be normal (Figure 4-2 A). However, in AIF deficient conditions, mtDNA replication still increases during the cell cycle but mtDNA degradation is not facilitated, which would lead to increased mtDNA copy number over time (Figure 4-2 B). Under these conditions, the mtDNA repair pathways should be highly active, given that more mtDNA molecules need to be maintained (Figure 4-2 B).

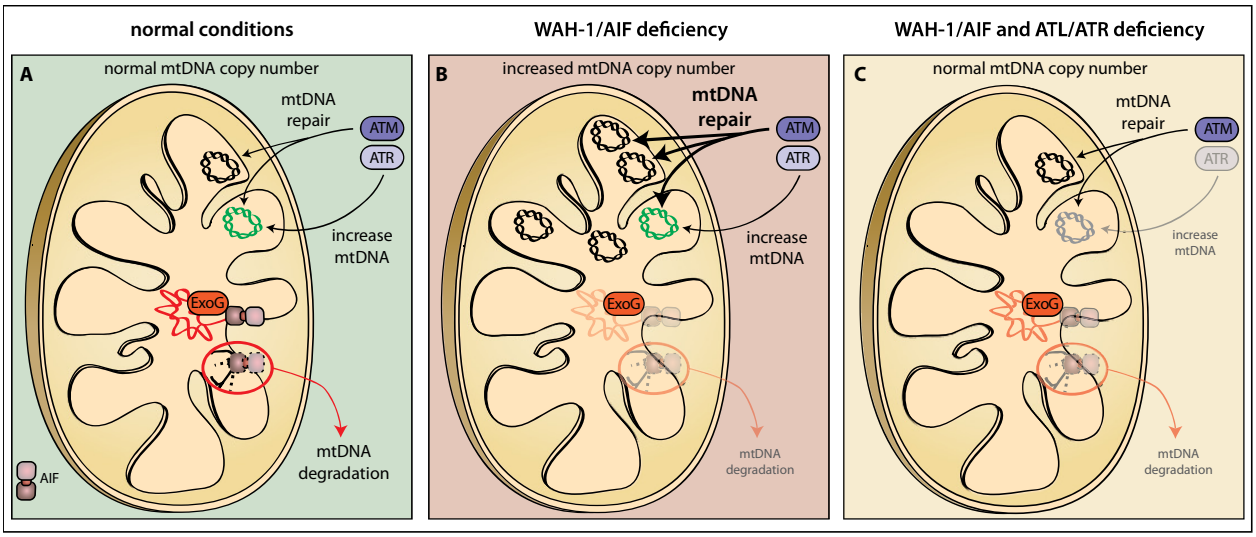


**Figure 4-2: Proposed working model of increased mtDNA copy number in AIF deficient conditions. A** Regulation of mtDNA under normal conditions. ATL-1/ATR activity leads to increased mtDNA in coordination with the cell cycle and AIF assists in degrading defective mtDNA molecules, which results in a balanced mtDNA turnover. **B** Regulation of mtDNA in AIF deficient conditions. ATL-1/ATR activity leads to increased mtDNA copy number and mtDNA degradation is impaired by AIF deficiency. This results in accumulation of mtDNA and increased activation of DNA repair pathways. **C** Regulation of mtDNA in AIF and ATL-1/ATR deficient conditions. ATL-1/ATR signaling that leads to increased mtDNA is impaired as well as mtDNA degradation is reduced. This results in normal mtDNA levels.

Deficiency of both AIF and ATR/*atl-1* might lead to disruption of the cell cycle dependent mtDNA replication signal therefore replication occurs only on a basal level (Figure 4-2 C). At the same time mtDNA degradation is reduced. Consequently, mtDNA copy number as well as the repair response should be restored to normal levels (Figure 4-2 C). However, in this scenario the whole organism might be extremely affected given that not enough mtDNA molecules are produced during cell proliferation. In this context, it might be interesting to study the phenotype of nematodes defective for both WAH-1/AIF and ATR/*atl-1*. For instance, one could address whether increased mtDNA leads to mitochondrial CI impairment in WAH-1/AIF deficient animals.

*Finally, what does AIF do under physiological conditions?*

In the previous chapters I have described and discussed the involvement of AIF in the stabilization of the ETC as well as its ability to modulate mitochondrial morphology and mtDNA copy number. How can one integrate these multiple observations into a suitable working model?

AIF is a transmembrane protein with its majority facing the IMS (Susin et al., 1999). Given that AIF is involved in ETC stabilization, it might reside in the vicinity of the ETC either inside or close to cristae structures. Since AIF was shown to form a complex with OPA1 (Zanna et al., 2008) it is likely that AIF is localized at the borders of the crista structure, close to the mitochondrial inner membrane organization system (MINOS). In yeast, MINOS contains six different subunits: The core components Mitofilin/Fcj1, Mio10 and Mio27 as well as Aim5, Aim13, Aim37, which are involved in the inheritance of mtDNA (van der Laan et al., 2012). The MINOS connects the inner boundary membrane with the crista and engages interactions with the OM (van der Laan et al., 2012). Consequently, alterations of this complex lead on the one hand to aberrant cristae structure and on the other hand to the destabilization of mtDNA nucleoids, given that MINOS is important for the positioning of nucleoids close to the ETC (Itoh et al., 2013). In addition to MINOS, also AIF might directly bind, stabilize or facilitate degradation of mtDNA molecules (see Figure 4-3). AIF deficiency might result in the destabilization of nucleoids, which renders them inaccessible to translation and transcription. This might lead to enhanced mtDNA replication or reduced mtDNA degradation as a compensatory mechanism to ensure the presence of some functional mtDNA molecules in the vicinity of the ETC.

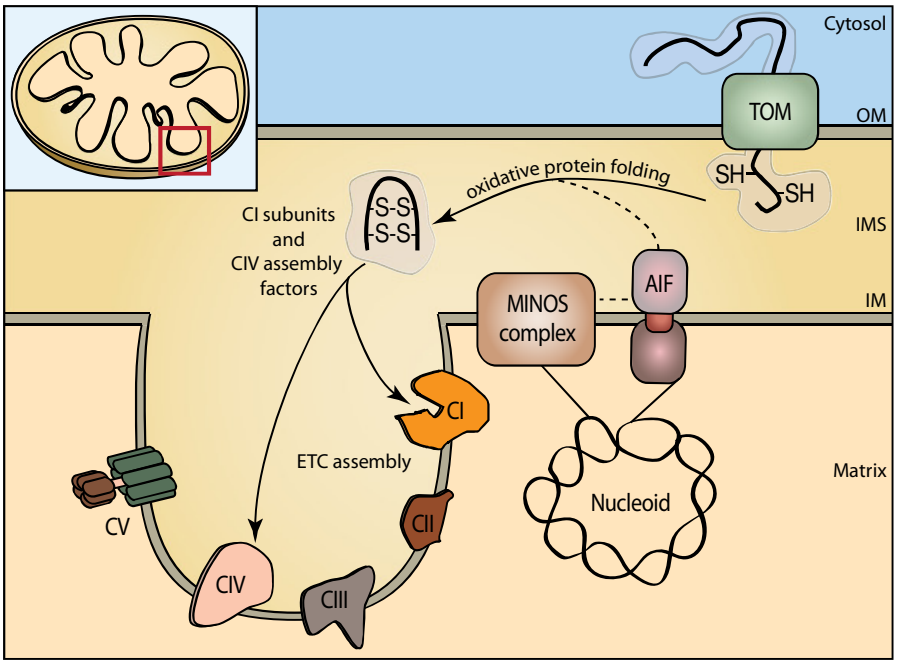


**Figure 4-3: Proposed function of AIF in mitochondria.** Unfolded intermembrane space (IMS) proteins are imported along the translocase of the outer membrane (TOM) complex. Oxidative protein folding leads to the formation of disulfide bonds and thereby proper folding of IMS proteins, such as CI subunits and CIV assembly factors, which leads to correct electron transport chain (ETC) assembly. The oxidoreductase activity of AIF assists in oxidative protein folding. Additionally, mtDNA nucleoids are tethered to the inner membrane (IM) through the mitochondrial inner membrane organization system (MINOS) and further stabilized by AIF.

Considering that the flavin moiety of AIF faces the IMS, the oxidoreductase activity of AIF could be important for redox-dependent processes in this compartment. A process, which requires oxidoreductases that might be catalyzed by AIF´s enzymatic activity, is oxidative protein folding (see Figure 4-3). In this process, unfolded mitochondrial IMS proteins that contain a twin-cysteine motif (twin-$CX_3C$ or twin-$CX_9C$) are imported via the TOM complex and folded by the formation of disulphide bonds in the IMS (Riemer et al., 2011). The formation of disulphide bonds is a rate-limiting step of the folding process and depends on the mitochondrial disulphide relay system, which channels two electrons away from the substrate protein to final electron acceptors (Riemer et al., 2011). In this context, AIF represents a suitable electron acceptor and might therefore assist in proper oxidative protein folding. In addition, AIF dimerises in the IM, which could serve for the efficient uptake of directly two electrons. Interestingly, among the IMS proteins that depend on oxidative folding are several subunits of CI and assembly factors for CIV (Cavallaro, 2010). These ETC components as well as assembly factors might be improperly folded in the absence of AIF, which could explain the ETC impairments observed in AIF deficient conditions.

This working hypothesis might be experimentally addressed by first demonstrating that AIF resides at the right location close to the cristae and second by assessing import and folding of proteins that depend on oxidative protein folding. To address whether AIF localizes close to both MINOS and the disulfide relay system, immunofluorescent colocalisation analysis can be conducted. Additionally, substrates of the mitochondrial disulfide relay system could be quantified by performing western blot analysis of isolated mitochondria derived from wildtype and harlequin mice cells.

## 5. Concluding remarks

Since its discovery in the context of apoptosis, AIF emerged as an indispensable protein for proper cellular function. It is involved in maintaining mitochondrial activity and dysfunction of AIF not only leads to severe phenotypes in mice but also results in devastating human diseases. Despite the importance of this protein for cellular viability, almost 20 years of AIF research could not clarify its actual function. The present study adds another layer of complexity to the already existing observations by demonstrating the involvement of AIF in the regulation of mtDNA copy number. This regulatory effect was independent of currently accepted pathways that regulate mtDNA content and further research is needed to discover the underlying mechanisms of this regulation. Given that depletion and mutation of mtDNA are the primary causes of mitochondrial disorders, the underlying pathways identified in this study might be important for understanding diseases associated with mitochondrial dysfunction and mightcontribute to the development of novel therapeutic strategies in the future.

## 6. List of Abbreviations

| Abbreviation | |
|---|---|
| ADP | Adenosine diphosphate |
| AIF | Apoptosis Inducing Factor |
| AMP | Adenosine monophosphate |
| ATL-1 | ATM (ataxia telangectasia mutated)-Like |
| ATM | Ataxia telangiectasia mutated |
| ATP | Adenosine triphosphate |
| ATR | Ataxia- and Rad-related |
| Bcl2 | B-cell lymphoma 2 |
| bZip | Basic leucine Zipper domain |
| C. elegans | Caenorhabditis elegans |
| CDC-25 | Cell Division Cycle related 25 |
| CDK-2 | Cyclin-Dependent Kinase 2 |
| Cdk5 | Cyclin-Dependent Kinase 5 |
| CHK2 | CHeckpoint Kinase 2 |
| CI | NADH dehydrogenase, complex I |
| CII | Succinate dehydrogenase, complex II |
| CIII | Cytochrome c reductase, complex III |
| CIV | Cytochrome c oxidase, complex IV |
| CLK-1 | CLocK (biological timing) abnormality |
| CNS | Central Nervous System |
| COXI | Cytochrome c oxidase I |
| COXIV | Cytochrome c oxidase IV |
| CPEO | Chronic progressive external ophthalmoplegia |
| CPS-6 | CED-3 Protease Suppressor |
| CV | F0F1-ATPase, complex V |
| CYE-1 | CYclin E |
| CypA | Cyclophilin A |
| Cyt B | Cytochrome B |
| Cyt c | Cytochrome c |
| D-loop | Displacement loop |
| DRP1 | Dynamin Related Protein 1 |
| dsDNA | Double stranded DNA |
| EAT-3 | EATing: abnormal pharyngeal pumping |
| EndoG | Endonuclease G |
| ESCs | Embryonic Stem Cells |
| ETC | Electron Transport Chain |
| ExoG | Endonuclease G-like 1 |
| FADH2 | Flavin Adenine Dinucleotide |
| FZO-1 | Fzo mitochondrial fusion protein |
| GAS-1 | General Anaesthetic Sensitivity abnormal |

| | |
|---|---|
| GLD-1 | defective in Germ Line Development |
| GLP-1 | abnormal Germ Line Proliferation 1 |
| GLP-4 | abnormal Germ Line Proliferation 4 |
| HCT116 | Human Colecteral Carcinoma cell line |
| Hep3B | Hepatocarcinoma cell line |
| HMG-5 | (high mobility group) box-containing protein 5 |
| Hmox1 | Heme oxygenase (decycling) 1 |
| Hsp70 | Heatshock Protein 70 |
| HSV-1 | Herpes simplex virus 1 |
| HU | Hydroxyurea |
| IMM | Inner mitochondrial membrane |
| IMS | Inner membrane space |
| KSS | Kearns-Sayre-Syndrome |
| LHON | Lebers hereditary optic neuropathy |
| MCF-7 | Michigan Cancer Foundation-7, breast cancer cell line |
| MDVs | Mitochondrial derived vesicles |
| MEF | Mouse embryonic fibroblasts |
| MELAS | mitochondrial encephalomyopathy, lactoacidosis and stroke like episodes |
| MERRF | myoclonic epilepsy with ragged red fibres |
| MEV-1 | abnormal MEthyl Viologen sensitivity |
| Mfn1 | Mitofusin 1 |
| Mfn2 | Mitofusin 2 |
| MGME1 | Mitochondrial genome maintenance exonuclease 1 |
| MINOS | Mitochondrial inner membrane organization system |
| MLS | Mitochondrial Localisation Sequence |
| MnSOD | Manganese superoxide dismutase |
| MPTP | Mitochondrial permeability transition pore |
| MRE-11 | Yeast MRE recombination/repair homolog |
| MTCO1 | Mitochondrial Cytochrome C Oxidase Subunit I |
| mtDNA | Mitochondrial DNA |
| mtRNA | Mitochondrial RNA |
| mtSSBP | Mitochondrial single stranded binding protein |
| NADH | Nicotinamide adenine dinucleotide |
| Ndufb8 | NADH dehydrogenase (ubiquinone) 1 beta subcomplex 8 |
| NLS | Nuclear Localisation Sequence |
| NRF | Nuclear respiratory transcription factors |
| OM | Outer mitochondrial Membrane |
| OPA1 | Optic atrophy 1 |
| OXPHOS | Oxidative phosphorylation |
| PARP | Poly(ADP-ribose) polymerase |
| PARylation | poly(ADP-ribosyl)ation |
| PCD | Programed cell death |
| PCNA | Proliferating cell nuclear antigen |
| PEST | Proline (P), glutamic acid (E), serine (S) and threonine (T) rich |

| | |
|---|---|
| PGC1α | Peroxisome proliferator-activated receptor gamma coactivator-1 α |
| PINK1 | PTEN-induced putative kinase protein 1 |
| PME-1 | Poly(ADP-ribose) Metabolism Enzyme 1 |
| PME-2 | Poly(ADP-ribose) Metabolism Enzyme 2 |
| POLG | Polymerase γ |
| qPCR | Quantitative real time PCR |
| RNAi | RNA interference |
| ROS | Reactive oxygen species |
| rRNAs | ribosomal RNAs |
| SKN-1 | SKiNhead |
| SOD | Superoxide dismutase |
| TFAM | Mitochondrial transcription factor A |
| TIM | Translocase of the inner mitochondrial membrane |
| TOM | Translocase of the outer mitochondrial membrane |
| tRNAs | transfer RNAs |
| WAH-1 | Worm AIF (apoptosis inducing factor) Homolog |

# 7. Material and Methods

## 7.1. *C. elegans* work

*C. elegans* strains were obtained from the *C*aenorhabditis Genetics Centre (CGC, University of Minnesota). The following strains were used in this study:

**Tab 7-1:** List of strains used in this study

| Strain | alleles |
|---|---|
| N2 Bristol | wildtype |
| TK22 | *mev-1(kn1)* |
| CW152 | *gas-1(fc21)* |
| CB4576 | *clk-1(e2519)* |
| DA631 | *eat-3(ad426);him(e1489)* |
| CU6372 | *drp-1(tm1108)* |
| CB4037 | *glp-1(e2141)* |
| SS104 | *glp-4(bn2)* |
| DW101 | *atl-1(tm853);nT1* |
| VC381 | *atm-1(gk186)* |
| RB814 | *cdk-5(ok626)* |
| AG151 | *cdc-25.1(nr2036)/dpy-5(e61)unc-13(e450)* |
| WS3455 | *chk-2(gk212)* |
| GS307 | *cye-1(ar95)dpy-5(e16)/unc-13(e51)* |
| TJ1 | *cep-1(gk138)* |
| | *cep-1(opIs198)* |
| RB1042 | *pme-1(ok988)* |
| VC1178 | *pme-2(ok344)* |
| VC1253 | *cps-6(ok1718)* |

*C. elegans* strains were maintained as described previously (Brenner, 1974). Briefly, nematodes were maintained on NGM plates containing OP50 bacteria as a food source. The plates are stored at 20°C if not indicated otherwise. The wildtype strain used in this study was N2 Bristol.

RNAi knockdown was achieved as previously described, by feeding worms with HT115 bacteria carrying either the empty control vector (L4440) or the RNAi clone from the Ahringer library (Kamath et al., 2003).

### 7.1.1 Measurement of mtDNA copy number

MtDNA copy number was determined as described previously by Bratic et al. (Bratic et al., 2009).

Worms were synchronized by sodium-hydroxide bleaching to isolate C. elegans eggs. Eggs were plated on NGM plates and worms were allowed to develop until finishing their egg-laying phase (for N2 at day 12). Total worm DNA (see 3.2.1.) was extracted and subjected to RT-PCR to measure mtDNA copy number (see 3.2.5.)

## 7.2. Molecular Biology

### 7.2.1. DNA extraction

DNA for PCR, Southern Blot and mtDNA measurement was extracted using a standard isopropanol precipitation protocol. Cells and tissues were lysed in lysis buffer (100 mM Tris pH 8; 5 mM EDTA; 200 mM NaCl; 0.2% SDS), supplemented with 1 mg/ml Proteinase K for either 1-4 hours or overnight at 56°C. After complete lysis the sample was centrifuged for 20 minutes at 10000 rpm. For precipitation of DNA one volume of isopropanol was added to the lysate, DNA was pelleted by centrifugation (20 minutes 10000rpm) and afterwards washed with 200 µl of ethanol. Finally, the DNA was dried at 37°C until residual ethanol evaporated and resuspended in TE-4 buffer (10mM Tris pH 8; 0,1mM EDTA pH 8). For mtDNA measurement, 20 worms were lysed in 20 µl of worm lysis buffer (20 mM Tris pH 7.5; 50 mM EDTA; 200 mM NaCl; 0.5% SDS), supplemented with 1 mg/ml Proteinase K for one hour at 56°C and Proteinase K was heat inactivated at 85°C for 10 minutes. Subsequently the lysate was diluted 5 times by adding DNAse free H2O.

### 7.2.2. PCR and PCR-product purification

PCR for genotyping nematodes was carried out using Taq DNA Polymerase with Standard Taq Buffer (NEB), while amplification of mtDNA fragments for gel retardation assays and southern blot probes was carried out using the proofreading Phusion High-Fidelity DNA Polymerase (Thermo Scientific) using the manufacturer´s protocols. Extraction of PCR-products was performed by using the QIAquick PCR Purification Kit (Quiagen).

### 7.2.3. Southern Blot

Southern Blot analysis was used to determine the quality of mtDNA derived from nematodes and harlequin mice. Briefly, total DNA was digested with a suitable restriction enzyme, electrophoreticaly separated on an agarose gel, blotted onto a nylonmembrane and hybridized with a radiolabeled specific probe for mtDNA.

The restriction enzyme digestion of nematode mtDNA was performed by using the enzymes HindIII and XbaI, while mouse mtDNA was digested with the enzymes HindIII and SacI. To this end, a total amount of 10µg DNA from both species was digested in a water bath at 37°C over night. The restriction digestion reaction composed of template DNA, the restriction enzyme, restriction enzyme specific buffer, 1mM DTT, 1mM Spermidin and BSA in a total volume of 50µl. Subsequently the reaction was loaded onto a 0,7% agarose gel and separated over night at 28-32 V.

Next, the gel was depurinated for 10 min in 0,125M HCl and denatured in transferbuffer (0,5M NaOH, 1,5M NaCl) for 20 minutes. The fragments were transferred to a nylon membrane by capillary force over night. The membrane was washed in SCC buffer (15 mM NaCl; 1,5 mM Na-Citrat; pH 7.0) and DNA was fixed by baking the membrane for 2 hours at 80°C.

The radioactive labeling of mtDNA specific DNA probes with [α-32P]dCTP was carried out using the manufacturer´s instruction (Redprime II Random Labeling-Kit). To wash out excess [α-32P]dCTP the labeled oligonucleotides were purified on a Sephadex-column (Probe Quant G50 micro columns). Finally the probe was denatured at 95°C for 5 min, cooled on ice and added to the pre-hybridisation buffer (0.5 M $NaH_2PO_4$ pH 7; 7% (w/v) SDS; 1 mM EDTA pH 8.0; 0.5 mg/ml Salm-Sperm-DNA)

Before hybridisation, free binding sites were saturated by washing the membrane with SSC buffer and subsequent incubation with pre-hybridisation buffer (0.5 M $NaH_2PO_4$ pH 7; 7% (w/v) SDS; 1 mM EDTA pH 8.0; 0.5 mg/ml Salmon-Sperm-DNA solution) for 2h at 67°C in a glass tube. Salmon sperm DNA was denatured for 10 min at 95°C and the radioactive labeled probe was added to the buffer. Hybridisation was carried out over night at 64°C. For signal visualisation the membrane was covered with an autoradiographic film, which was developed afterwards.

### 7.2.4. RNA isolation

Prior to use, tissues, cells and nematodes were snapfrozen in liquid nitrogen and stored at -80°C. Total RNA isolation was performed using the QIAshredder (Qiagen) and RNeasy RNA isolation kit

(Qiagen) according to the manufacturer´s protocol. For RNA isolation from tissues a standard phenol-chloroform extraction was applied prior to using the RNeasy RNA isolation kit. Briefly, tissue was roughly homogenized in QIAazol reagent and loaded on a QIAshredder column. The flow-through was supplemented with 1/5 volume of chloroform, loaded on a phase lock gel heavy tube (Eppendorf), thoroughly mixed and centrifuged for 5 minutes at 10000 rpm. 1 Volume of 70% ethanol was added to the clear upper phase, loaded onto the RNeasy column and RNA was then isolated according to the manufacturer´s protocol. After isolation, RNA concentration was determined using the NanoDrop 2000c/2000 UV-Vis Spectrophotometer (Thermo Scientific).

### 7.2.5. Quantitative Real Time PCR (RT-PCR)

Expression level of several genes and determination of mtDNA copy number were assessed by quantitative real time PCR. For gene expression experiments 50-200ng of total RNA was reversed transcribed using qScript cDNA Synthesis Kit (Quanta Biosciences) following the manufacturer's protocol. For mtDNA copy number determination total DNA was used as a template.The PCR reaction was carried out in a Step One Plus Real time PCR System (Applied Biosystems) using the Fast SYBR Green Master Mix (Applied Biosystems). The following cycling conditions were used: Initial AmpliTaq Polymerase activation at 95°C for 20s followed by 40 cycles of denaturation (95°C for 3s) and Annealing/Extension (60°C for 30s). An average of at least 3 technical repeats was used for each biological data point and data was analysed using the comparative ΔΔCt method (Livak and Schmittgen, 2001).

**Table 7-2:** Primer sequences used in this study

| Target | Sequence |
|---|---|
| *beta-actin* | 5´-tgtgatgccagatcttctccat-3´ and 5´-gagcacggtatcgtcaccaa-3´ |
| *wah-1* | 5´-gctgatgctgtcgaggaga-3´and 5´-tggtggtgttctcttctgtaga-3´ |
| *chk-1* | 5'-ctctggcggagagacagaat -3' and 5'-cattcgttggaggagattcg -3' |
| *par-2.1* | 5'-ctaccgtccgctgtatgtca -3' and 5'-ggtttttcagcgaacaagtca -3' |
| *hmg-5* | 5´-gcattcactgattcccagaaa-3` 5´-tttctttctgttcggcttcc-3` |
| *cps-6* | 5'-tgagcaatatgagccacaa -3' and 5'-gggaccggtgattatgtagg -3' |
| *eat-3* | 5'-aggatcaaaatggaaattcagg -3' and 5'-catcaatgaggcgagaatga -3' |

| | |
|---|---|
| *fzo-1* | 5'-ggggatgtctatggagaactga -3' and 5'-ccgctgttcagaactaacaaagt -3' |
| *dve-1* | 5'-gcattcagcacccactca-3' and 5'-gagtgggtcgaacatcagg-3' |
| | *C. elegans* mitochondrial genes |
| *COX1* | 5′-tgggttgacaggtgttgtattatct -3′ and 5′-gtgtaacacccgtgaaaatcc -3′ |
| *ND1* | 5′-agcgtcatttattgggaagaagac -3′ and 5′-aagcttgtgctaatcccataaatgt -3′ |
| *ND4* | 5′-aggctcctacaacagctagaatactt -3′ and 5′-gcaattaaaattcatacattgttgtgt -3′ |
| *COX3* | 5′-gacgggtttaaattcggagtaa -3′ and 5′-tctcccaactcgtgtactggt -3′ |
| Mouse Primers for mRNA detection by RT-PCR | |
| HMOX | 5′-ggagcctgaatcgagcagaa -3′ and 5′-tcagcattctcggcttggat -3′ |
| Nrf1 | 5′-cggcagctgatgaggtaac -3′ and 5′-tttccgtttcttcttccctgttg -3′ |
| Nrf2 | 5′-catgatggacttggagttgc -3′ and 5′-cctccaaaggatgtcaatcaa -3′ |
| SOD2 | 5′-tgctctaatcaggacccattg -3′ and 5′-gtagtaagcgtgctcccacac -3′ |
| Ndufs8 | 5′-catcggctcttggctcag -3′ and 5′-ttgcctgcaaactctgtgag -3′ |
| Atp5a1 | 5′-gctgaggaatgttcaagcaga -3′ and 5′-ccaagttcagggacataccc -3′ |
| SDHb | 5′-ctggtggaacggagacaagt -3′ and 5′-gcgttcctctgtgaagtcgt -3′ |
| Uqcrc1 | 5′-cgcacagattgactgactacc -3′ and 5′-caagtgtttctgggcaaggt -3′ |
| TFAM | 5′-caaaggatgattcggctcag -3′ and 5′-aagctgaatatatgcctgctttc -3′ |
| | Mouse mitochondrial genes |
| *ND6* | 5′-cacaactatatattgccgctaccc -3′ and 5′-tggtttgggagattggttg -3′ |
| *ND5* | 5′-agcattcggaagcatctttg -3′ and 5′-ttgtgaggactggaatgctg -3′ |
| *ND1* | 5′-caaacacttattacaacccaagaaca -3′ and 5′-tcatattatggctatgggtcagg -3′ |
| *COX1* | 5′-cagccgcaacctaaacaca -3′ and 5′-ttctgggtgcccaaagaat -3′ |
| *ND4L* | 5′-caactccataagctccatacca -3′ and 5′-gctagttcctacagctgcttcg -3′ |
| *CYTB* | 5′-catttattatcgcggcccta -3′ and 5′-tgggttgtttgatcctgtttc -3′ |
| | *C. elegans* primers for assessing mtDNA copy number |
| actin | 5′-ggtggttcctccggaaagaa -3′ and 5′-tgcgacattgatatccgtaagg -3′ |
| nd-1 | 5′-agcgtcatttattgggaagaagac -3′ and 5′-aagcttgtgctaaatcccataaatgt -3′ |
| | mouse primers for assessing mtDNA copy number |
| actin | 5′-ggaaaagagcctcagggcat -3′ and 5′-gaagagctatgagctgcctga -3′ |
| nd-2 | 5′-cccattccacttctgattacc -3′ and 5′-atgatagtagagttgagtagcg -3′ |
| | human primers for assessing mtDNA copy number |
| actin | 5′-ccacctcagtcttcccatct -3′ and 5′-ctttctctctgccctgatcc -3′ |

| | |
|---|---|
| h_mtDNA (3212-3299) | 5′-cacccaagaacagggtttgt -3′ and 5′-tggccaatgggtatgttgttaa -3′ |
| | Mouse mtDNA Fragment primer for gel retardation assay |
| D-loop/12S 1128bp | F(15311-15334) 5′- ctctggtcttgtaaacctgaaatg-3′<br>R(11170-11190) 5′- caccggtctatggaggtttgc-3′ |
| COXI, COXII,ATP8 1242bp | F(6628-6647) 5′-caggaataccacgacgctac -3′<br>R(7847-7868) 5′-gtgggaatgtttgtgatgagac -3′ |
| COXI, COXII,ATP8, COXIII 2707bp | F(6628-6647) 5′-caggaataccacgacgctac -3′<br>R(9312-9333) 5′-gtcgcagttgaatgctgtgtag -3′ |
| ND4, ND5 1501bp | F(11170-11190) 5′-gaacggatccacagccgtact -3′<br>R(12649-12670) 5′-gttggcttgatgtagagaaggc -3′ |
| ND4, ND5, ND6 2929bp | F(11170-11190) 5′-gaacggatccacagccgtact -3′<br>R(14077-14098) 5′-gtcgcagttgaatgctgtgtag -3′ |
| *C. elegans* primers for Southern Blot probes | |
| Probe_celegans | F(12082-12105) 5′- cagcattaactaatcgtctaggtg -3′<br>R(12591-12615) 5′- catcttgttgtccaaatgaacaatg -3′ |
| mouse primers for Southern Blot probes | |
| Probe_mouse | F(9312-9333) 5′- gaagccgcagcatgatactgac -3′<br>R(10089-10109) 5′- gtagggctagtcctacagctg -3′ |

## 7.3. Cell Biology

### 7.3.1. Culturing of cell lines and mouse embryonic fibroblasts (MEF)

Cell lines (HEK293T, HeLa, 3T3 and SH-SY5Y) and MEF cells were cultured in DMEM (Life Technologies) supplemented with 1% Penicillin/Streptomycin (Life Technologies) and 10% fetal calf serum (FCS) (Life Technologies) at 37°C under 5% CO2 atmosphere. Cells were passaged by trypsinisation every 2-3 days. Briefly, cell culture media was aspirated, cells were washed once with PBS and incubated with a suitable volume of trypsin solution (Life Technologies). After detachment of

cells, trypsin was inactivated by adding the same volume of complete DMEM media and pelleted by centrifugation for 2 min at 1000g. Subsequently cells were resuspended in complete DMEM and plated on a fresh cell culture dish for further cultivation.

### 7.3.2. Freezing and thawing of cells

Cell lines (HEK293T, HeLa, 3T3 and SH-SY5Y) were trypsinised, pelleted and resuspended in 4°C cold freezing medium (DMEM, 1% Penicilin/Streptomycin, 10% FCS, 10% DMSO), while MEF cells were resuspended in FCS supplemented with 10% DMSO. The cryotubes were transferred to -80°C in a Mr. Frosty Freezing Container (Thermo Scientific) to ensure a cooling of -1°C/minute. For long term storage cells were transferred to liquid nitrogen.

Cells were thawed by transferring cryotubes to a water bath at 37°C. The thawed cells were resuspended in 5 ml of complete pre-warmed DMEM, pelleted, resuspended in complete DMEM and directly plated.

### 7.3.3. Preparation and culturing of primary cell culture

Primary cell cultures were prepared with the help of Mrs. Bartling-Kirsch and Dr. Jakubik.

#### *7.3.3.1. Mouse embryonic fibroblast cells*

MEFs were prepared at embryonic day E13.5-E15.5 from wildtype (wt/Y) and harlequin (Hq/Y) littermates. Briefly, embryos were removed from the uterus of pregnant mice and liver and heart were removed, the head was kept for subsequent genotyping of the embryos. The remaining parts of the embryos were chopped in 1.5 ml PBS and mixed with 30-40ml Trypsin. The crude tissue was further trypsinised by stirring at 37°C and the reaction was stopped by adding 30 ml EF medium (DMEM, 1% Penicillin/Streptomycin, 10% FCS, 250 µg/ml Amphotericin B). The cell mixture was passed through a cell strainer, pelleted for 10 min at 1200 rpm and resuspended in 10 ml EF medium. Finally, the cell number was determined and $5x10^6$ cells were plated on gelatin coated 15 cm cell culture dishes (0.1% gelatine). Culturing of MEF cells was performed as previously described.

### 7.3.4. Differentiation of SHSY5Y cells

In order to differentiate SH-SY5Y cells, 50 μM of retinoic acid was added to the standard cell culture medium. Differentiation can be observed 5 days after supplementation. Cells were allowed to stay in culture for another 2 days and then collected for western blotting.

## 7.4. Biochemistry

### 7.4.1. Protein isolation

Cells, tissues and nematodes were homogenized and lysed on ice in RIPA buffer (radioimmuno precipitation assay buffer) supplemented with protease- (cOmplete Protease Inhibitor Cocktail Tablets, Roche) and phosphatase inhibitors (PhosSTOP Phosphatase Inhibitor Cocktail Tablets, Roche). Cell debris were pelleted by centrifugation for 5 min at 10000g, the supernatant was transferred to a fresh tube and protein concentration was determined by Bradford protein assay (Biorad).

### 7.4.2. Western Blot

Proteins from cells, tissues and nematodes were separated by SDS polyacrylamide gel electrophoresis (SDS-PAGE). Briefly, 4x Laemmli buffer (250mM Tris/HCl pH 6.8, 8% SDS, 40% glycerol, 20% β-mercaptoethanol, 1mg/ml bromphenolblue) was added to 30 μg of total protein. The samples was loaded onto a polyacrylamide gel and allowed to pass through the stacking gel by applying a current of 80mV for 20 min. The current was then increased to 130 mV until the proteins reached the desired state of separation. Proteins were transferred to a nitrocellulose membrane by wetblotting for 90 min at 300 mA. The membrane was briefly washed with TBST buffer (15.3mM Tris/HCl, 140mM NaCl, pH 7.6, 0,1% Tween) and unspecific binding was blocked by incubation with 5% nonfat milk powder in TBST-buffer for 30 minutes. After blocking the primary antibody was diluted in 5% milk-TBST and incubated with the membrane either over night at 4°C or 1-2 hours at room temperature. The antibody was removed by washing the membrane 3 times for 10 minutes with TBST-buffer. The secondary (horseradish peroxidase conjugated, HRP) antibody was diluted 1:8000 in 5% milk-TBST and incubated with the membrane for 45 minutes. The membranes were washed 3 times with TBST and finally developed with peroxidase substrate for enhanced chemiluminescence (Pierce ECL

Western Blotting Substrate, Thermo Scientific) according to the manufacturer´s instructions. The chemiluminescence detection was performed using the ChemiDoc XRS+ Gel documentation system (BioRad).

Antibodies used in this study are listed in the table below:

**Table 7-3:** List of antibodies used in this study for Western Blot (WB) or Immuncytochemistry (IC)

| Antibody | Host | Company | Application |
|---|---|---|---|
| Anti-AIF | Rabbit polyclonal | Millipore AB16501 | WB |
| Anti-Alpha-Tubulin | Mouse monoclonal | Sigma (T8203) | WB |
| Anti-MT-ND5 (Complex I) | Rabbit monoclonal | MitoSciences | WB |
| Anti-MT-CO3 (Complex III) | Mouse monoclonal | MitoSciences | WB |
| Anti-DRP-1 (D6C7) | Rabbit monoclonal | Cell Signaling (8570) | WB |
| Anti-Mitofilin | Mouse monoclonal | MitoSciences (ab110329) | WB |
| Anti-Ndufa9 (Complex I) | Mouse monoclonal | MitoSciences | WB |
| Anti-Ndufs4 (Complex I) | Mouse monoclonal | MitoSciences | WB |
| Anti-SDHA (Complex II) | Mouse monoclonal | MitoSciences | WB |
| Anti-TFAM | Rabbit polyclonal | Calbiochem | WB |
| Anti-ATP synthase subunit alpha | Mouse monoclonal | MitoSciences, MS507 | WB |
| Anti-Ndufs3 (Complex I) | Mouse monoclonal | MitoSciences, MS112 | WB |
| Anti-MT-CO1 (Complex IV) | Mouse monoclonal | MitoSciences, MS404 | WB |
| Anti-COX (mtDNA encoded) | Rabbit polyclonal | Cell Signaling | WB |
| Anti-COXIV(nuclear encoded) | Rabbit polyclonal | Cell Signaling | WB |
| Anti-CyclinE (M20) | Rabbit polyclonal | Santa Cruz | WB |
| Anti-Mitofusin-1 | Rabbit polyclonal | Millipore (ABC41) | WB |
| Anti-OPA1 | Mouse monoclonal | BD bioscience (612606) | WB |
| Anti-PARP | Rabbit polyclonal | Cell Signaling | WB |
| Anti-TOM20 | Rabbit polyclonal | SantaCruz (sc-11415) | WB/IC |
| Total OXPHOS Rodent WB Antibody Cocktail | Mouse polyclonal | Abcam (ab110413) | WB |

### 7.4.3. Propidium Iodide (PI) staining for cell cycle analysis and fluorescence activated cell scanning (FACS)

MEF cells collected for PI staining were cultured as previously described. At least $1x10^6$ cells were washed once with PBS, pelleted and resuspended in 100µl ice cold PBS. In order to fix the cells, 900µl of ice-cold 70% ethanol were added to the cell suspension drop-wise while vortexing. Finally, the samples were transferred to -20°C for at least 2h to finalize the fixation process. Fixed samples were stored at -20°C until PI staining was performed. Cells were initially washed 2-3 times with PBS until ethanol was removed and pelleted at 1200 rpm for 10 min. Subsequently they were resuspended in 50 µl 1mg/ml RNAse and 300µl of PI staining solution (0.1% Triton X-100, 500µg/ml PI) was added. The samples were transferred to FACS tubes, protected from light and incubated with the staining solution for 20 min at room temperature on a shaker. Finally, flow cytometry analysis was performed, using the Gallios Beckmann Coulter flow cytometer.

## 7.5. Microscopy

### 7.5.1. Staining for Live-Cell imaging

MEF cells were plated on glass bottom culture dishes for microscopy and cultured as previously described. For live imaging of mitochondria, cells were incubated for 10 min with 100 nM Mitotracker (MitoTracker Green FM, Invitrogen). After incubation with Mitotracker, cells were washed once with dye-free cell culture medium and finally imaged.

### 7.5.2. Measurement of mitochondrial morphology

Mitochondrial morphology in MEF cells was assessed with the Andor Spinning Disk microscope. The system comprises a fully motorized inverted Nikon microscope in association with a Yokogawa Spinning Disk connected to a back-illuminated EMCCD camera (Andor iXON DU-897, 512 x 512 pixels, 16 bit, 35 frames/sec). The setup was equipped with a 100x oil-immersion lens (Nikon). Fluorescence was measured at 490 nm excitation and a 516 nm emission filter. The analysis included 15 images from 4 different MEF cell clones for each genotype (wildtype and harlequin). Image analysis of mitochondrial length and number of mitochondrial branches was performed using the Fiji image processing software.

## 7.6. List of Buffers

**Table 7-4:** List of Buffers used in this study

| Buffer | Composition |
|---|---|
| NGM (nematode growth media) | 3 g NaCl, 17 g agar, 2.5 g peptone, 1 ml cholesterol in 1l H2O, after autoclaving 1 ml of 1M CaCl2, 1 ml of 1 M MgSO4 and 25 ml of 1M KPO4 are added |
| LB | 10 g Bacto-tryptone, 5 g Bacto-yeast , 5 g NaCl up to 1 l with dH2O adjusted to pH 7.0 using 1 M NaOH |
| M9 | 3 g KH2PO4, 6 g Na2HPO4, 5 g NaCl, 1 ml 1M MgSO4 up to 1 l with dH2O |
| **Buffer Molecular Biology** | |
| DNA Lysis Buffer | 100 mM Tris pH 8; 5 mM EDTA; 200 mM NaCl; 0.2% SDS |
| Worm DNA Lysis Buffer | 20 mM Tris pH 7.5; 50 mM EDTA; 200 mM NaCl; 0.5% SDS |
| TE-4 Buffer | 10mM Tris pH 8; 0,1mM EDTA pH 8 |
| Southern Blot Transfer buffer | 0,5M NaOH, 1,5M NaCl |
| Southern Blot SCC buffer | 15 mM NaCl; 1,5 mM Na-Citrat; pH 7.0 |
| Southern Blot Pre-Hybridisation buffer | 0.5 M $NaH_2PO_4$ pH 7; 7% (w/v) SDS; 1 mM EDTA pH 8.0; 0.5 mg/ml salmon-sperm-DNA |
| **Buffer Cell Culture** | |
| Complete cell cuture media | DMEM(high glucose, pyruvate, L-glutamine), 1% Penicilin/Streptomycin, 10% FCS |
| Freezing media | DMEM(high glucose, pyruvate, L-glutamine), 1% penicilin/streptomycin, 10% FCS, 10% DMSO |
| EF medium | DMEM, 1% penicillin/streptomycin, 10% FCS, 250 µg/ml Amphotericin B |
| HBSS 2x buffer | 50mM HEPES, 10mM KCl, 280nM NaCl, 1.5mM Na2HPO4 |
| **Buffer Biochemistry** | |
| Lower Buffer WB | 1.5M Tris-Base, 0.4% SDS, pH 8.8 |
| Upper Buffer WB | 1M Tris-Base, 0.4% SDS, pH 6.8 |
| Transfer and Electrophoresis buffer | 25mM Tris-Base, 192mM glycine |
| 10x TBS Buffer | 153mM Tris-HCl, 1.4M NaCl, pH 7.6 |

| | |
|---|---|
| TBST buffer | 15.3mM Tris/HCl, 140mM NaCl, pH 7.6, 0,1% Tween |
| Laemmli Buffer | 250mM Tris/HCl pH 6.8, 8% SDS, 40% glycerol, 20% β-mercaptoethanol, 1mg/ml bromphenolblue |

## 8. References


Achanta G, Sasaki R, Feng L, Carew JS, Lu W, Pelicano H, Keating MJ, Huang P (Novel role of p53 in maintaining mitochondrial genetic stability through interaction with DNA Pol gamma. EMBO J 24:3482-3492.2005).

Agholme L, Lindstrom T, Kagedal K, Marcusson J, Hallbeck M (An in vitro model for neuroscience: differentiation of SH-SY5Y cells into cells with morphological and biochemical characteristics of mature neurons. J Alzheimers Dis 20:1069-1082.2010).

Aguer C, Gambarotta D, Mailloux RJ, Moffat C, Dent R, McPherson R, Harper ME (Galactose enhances oxidative metabolism and reveals mitochondrial dysfunction in human primary muscle cells. PLoS One 6:e28536.2011).

Al Rawi S, Louvet-Vallee S, Djeddi A, Sachse M, Culetto E, Hajjar C, Boyd L, Legouis R, Galy V (Postfertilization autophagy of sperm organelles prevents paternal mitochondrial DNA transmission. Science 334:1144-1147.2011).

Allsopp TE, Wyatt S, Paterson HF, Davies AM (The proto-oncogene bcl-2 can selectively rescue neurotrophic factor-dependent neurons from apoptosis. Cell 73:295-307.1993).

Alvira D, Ferrer I, Gutierrez-Cuesta J, Garcia-Castro B, Pallas M, Camins A (Activation of the calpain/cdk5/p25 pathway in the girus cinguli in Parkinson's disease. Parkinsonism Relat Disord 14:309-313.2008).

Apostolova N, Cervera AM, Victor VM, Cadenas S, Sanjuan-Pla A, Alvarez-Barrientos A, Esplugues JV, McCreath KJ (Loss of apoptosis-inducing factor leads to an increase in reactive oxygen species, and an impairment of respiration that can be reversed by antioxidants. Cell Death Differ 13:354-357.2006).

Armand AS, Laziz I, Djeghloul D, Lecolle S, Bertrand AT, Biondi O, De Windt LJ, Chanoine C (Apoptosis-inducing factor regulates skeletal muscle progenitor cell number and muscle phenotype. PLoS One 6:e27283.2011).

Artus C, Boujrad H, Bouharrour A, Brunelle MN, Hoos S, Yuste VJ, Lenormand P, Rousselle JC, Namane A, England P, Lorenzo HK, Susin SA (AIF promotes chromatinolysis and caspase-independent programmed necrosis by interacting with histone H2AX. EMBO J 29:1585-1599.2010).

Ashcroft NR, Srayko M, Kosinski ME, Mains PE, Golden A (RNA-Mediated interference of a cdc25 homolog in Caenorhabditis elegans results in defects in the embryonic cortical membrane, meiosis, and mitosis. Dev Biol 206:15-32.1999).

Ban-Ishihara R, Ishihara T, Sasaki N, Mihara K, Ishihara N (Dynamics of nucleoid structure regulated by mitochondrial fission contributes to cristae reformation and release of cytochrome c. Proc Natl Acad Sci U S A 110:11863-11868.2013).

Benit P, Goncalves S, Dassa EP, Briere JJ, Rustin P (The variability of the harlequin mouse phenotype resembles that of human mitochondrial-complex I-deficiency syndromes. PLoS One 3:e3208.2008).

Berger I, Ben-Neriah Z, Dor-Wolman T, Shaag A, Saada A, Zenvirt S, Raas-Rothschild A, Nadjari M, Kaestner KH, Elpeleg O (Early prenatal ventriculomegaly due to an AIFM1 mutation identified by linkage analysis and whole exome sequencing. Mol Genet Metab 104:517-520.2011).

Bogenhagen DF (Mitochondrial DNA nucleoid structure. Biochim Biophys Acta 1819:914-920.2012).

Braschi E, Goyon V, Zunino R, Mohanty A, Xu L, McBride HM (Vps35 mediates vesicle transport between the mitochondria and peroxisomes. Curr Biol 20:1310-1315.2010).

Bratic I, Hench J, Henriksson J, Antebi A, Burglin TR, Trifunovic A (Mitochondrial DNA level, but not active replicase, is essential for Caenorhabditis elegans development. Nucleic Acids Res 37:1817-1828.2009).

Brauchle M, Baumer K, Gonczy P (Differential activation of the DNA replication checkpoint contributes to asynchrony of cell division in C. elegans embryos. Curr Biol 13:819-827.2003).
Brenner S (The genetics of Caenorhabditis elegans. Genetics 77:71-94.1974).
Brown D, Yu BD, Joza N, Benit P, Meneses J, Firpo M, Rustin P, Penninger JM, Martin GR (Loss of Aif function causes cell death in the mouse embryo, but the temporal progression of patterning is normal. Proc Natl Acad Sci U S A 103:9918-9923.2006).
Burkle A, Virag L (Poly(ADP-ribose): PARadigms and PARadoxes. Mol Aspects Med 34:1046-1065.2013).
Cavallaro G (Genome-wide analysis of eukaryotic twin CX9C proteins. Mol Biosyst 6:2459-2470.2010).
Chatre L, Ricchetti M (Prevalent coordination of mitochondrial DNA transcription and initiation of replication with the cell cycle. Nucleic Acids Res 41:3068-3078.2013).
Chen H, Vermulst M, Wang YE, Chomyn A, Prolla TA, McCaffery JM, Chan DC (Mitochondrial fusion is required for mtDNA stability in skeletal muscle and tolerance of mtDNA mutations. Cell 141:280-289.2010).
Cheung EC, Joza N, Steenaart NA, McClellan KA, Neuspiel M, McNamara S, MacLaurin JG, Rippstein P, Park DS, Shore GC, McBride HM, Penninger JM, Slack RS (Dissociating the dual roles of apoptosis-inducing factor in maintaining mitochondrial structure and apoptosis. EMBO J 25:4061-4073.2006).
Cheung EC, Melanson-Drapeau L, Cregan SP, Vanderluit JL, Ferguson KL, McIntosh WC, Park DS, Bennett SA, Slack RS (Apoptosis-inducing factor is a key factor in neuronal cell death propagated by BAX-dependent and BAX-independent mechanisms. J Neurosci 25:1324-1334.2005).
Chin GM, Villeneuve AM (C. elegans mre-11 is required for meiotic recombination and DNA repair but is dispensable for the meiotic G(2) DNA damage checkpoint. Genes Dev 15:522-534.2001).
Chinta SJ, Rane A, Yadava N, Andersen JK, Nicholls DG, Polster BM (Reactive oxygen species regulation by AIF- and complex I-depleted brain mitochondria. Free Radic Biol Med 46:939-947.2009).
Chung SH, Calafiore M, Plane JM, Pleasure DE, Deng W (Apoptosis inducing factor deficiency causes reduced mitofusion 1 expression and patterned Purkinje cell degeneration. Neurobiol Dis 41:445-457.2011).
Cote C, Boulet D, Poirier J (Expression of the mammalian mitochondrial genome. Role for membrane potential in the production of mature translation products. J Biol Chem 265:7532-7538.1990).
Cote J, Ruiz-Carrillo A (Primers for mitochondrial DNA replication generated by endonuclease G. Science 261:765-769.1993).
Cymerman IA, Chung I, Beckmann BM, Bujnicki JM, Meiss G (EXOG, a novel paralog of Endonuclease G in higher eukaryotes. Nucleic Acids Res 36:1369-1379.2008).
De los Rios Castillo D, Zarco-Zavala M, Olvera-Sanchez S, Pardo JP, Juarez O, Martinez F, Mendoza-Hernandez G, Garcia-Trejo JJ, Flores-Herrera O (Atypical cristae morphology of human syncytiotrophoblast mitochondria: role for complex V. J Biol Chem 286:23911-23919.2011).
De Stefani D, Raffaello A, Teardo E, Szabo I, Rizzuto R (A forty-kilodalton protein of the inner membrane is the mitochondrial calcium uniporter. Nature 476:336-340.2011).
DiMauro S (Mitochondrial diseases. Biochim Biophys Acta 1658:80-88.2004).
Doti N, Reuther C, Scognamiglio PL, Dolga AM, Plesnila N, Ruvo M, Culmsee C (Inhibition of the AIF/CypA complex protects against intrinsic death pathways induced by oxidative stress. Cell Death Dis 5:e993.2014).
Douglas PM, Dillin A (Protein homeostasis and aging in neurodegeneration. J Cell Biol 190:719-729.2010).

Duguay BA, Smiley JR (Mitochondrial nucleases ENDOG and EXOG participate in mitochondrial DNA depletion initiated by herpes simplex virus 1 UL12.5. J Virol 87:11787-11797.2013).
Edgar D, Trifunovic A (The mtDNA mutator mouse: Dissecting mitochondrial involvement in aging. Aging (Albany NY) 1:1028-1032.2009).
Eilers M, Oppliger W, Schatz G (Both ATP and an energized inner membrane are required to import a purified precursor protein into mitochondria. EMBO J 6:1073-1077.1987).
El-Hattab AW, Scaglia F (Mitochondrial DNA depletion syndromes: review and updates of genetic basis, manifestations, and therapeutic options. Neurotherapeutics 10:186-198.2013).
Falkenberg M, Larsson NG, Gustafsson CM (DNA replication and transcription in mammalian mitochondria. Annu Rev Biochem 76:679-699.2007).
Fernandez-Silva P, Enriquez JA, Montoya J (Replication and transcription of mammalian mitochondrial DNA. Exp Physiol 88:41-56.2003).
Ferreira P, Villanueva R, Martinez-Julvez M, Herguedas B, Marcuello C, Fernandez-Silva P, Cabon L, Hermoso JA, Lostao A, Susin SA, Medina M (Structural insights into the coenzyme mediated monomer-dimer transition of the pro-apoptotic apoptosis inducing factor. Biochemistry 53:4204-4215.2014).
Furda AM, Marrangoni AM, Lokshin A, Van Houten B (Oxidants and not alkylating agents induce rapid mtDNA loss and mitochondrial dysfunction. DNA Repair (Amst) 11:684-692.2012).
Geng Y, Yu Q, Sicinska E, Das M, Schneider JE, Bhattacharya S, Rideout WM, Bronson RT, Gardner H, Sicinski P (Cyclin E ablation in the mouse. Cell 114:431-443.2003).
Ghezzi D, Sevrioukova I, Invernizzi F, Lamperti C, Mora M, D'Adamo P, Novara F, Zuffardi O, Uziel G, Zeviani M (Severe X-linked mitochondrial encephalomyopathy associated with a mutation in apoptosis-inducing factor. Am J Hum Genet 86:639-649.2010).
Gkikas I, Petratou D, Tavernarakis N (Longevity pathways and memory aging. Front Genet 5:155.2014).
Glover-Cutter KM, Lin S, Blackwell TK (Integration of the unfolded protein and oxidative stress responses through SKN-1/Nrf. PLoS Genet 9:e1003701.2013).
Gomes LC, Di Benedetto G, Scorrano L (During autophagy mitochondria elongate, are spared from degradation and sustain cell viability. Nat Cell Biol 13:589-598.2011).
Gomez LA, Monette JS, Chavez JD, Maier CS, Hagen TM (Supercomplexes of the mitochondrial electron transport chain decline in the aging rat heart. Arch Biochem Biophys 490:30-35.2009).
Gouspillou G, Bourdel-Marchasson I, Rouland R, Calmettes G, Biran M, Deschodt-Arsac V, Miraux S, Thiaudiere E, Pasdois P, Detaille D, Franconi JM, Babot M, Trezeguet V, Arsac L, Diolez P (Mitochondrial energetics is impaired in vivo in aged skeletal muscle. Aging Cell 13:39-48.2014).
Gozuacik D, Kimchi A (Autophagy and cell death. Curr Top Dev Biol 78:217-245.2007).
Gross NJ, Getz GS, Rabinowitz M (Apparent turnover of mitochondrial deoxyribonucleic acid and mitochondrial phospholipids in the tissues of the rat. J Biol Chem 244:1552-1562.1969).
Gurbuxani S, Schmitt E, Cande C, Parcellier A, Hammann A, Daugas E, Kouranti I, Spahr C, Pance A, Kroemer G, Garrido C (Heat shock protein 70 binding inhibits the nuclear import of apoptosis-inducing factor. Oncogene 22:6669-6678.2003).
Hallberg BM, Larsson NG (TFAM forces mtDNA to make a U-turn. Nat Struct Mol Biol 18:1179-1181.2011).
Hansson A, Hance N, Dufour E, Rantanen A, Hultenby K, Clayton DA, Wibom R, Larsson NG (A switch in metabolism precedes increased mitochondrial biogenesis in respiratory chain-deficient mouse hearts. Proc Natl Acad Sci U S A 101:3136-3141.2004).
Harper JW, Elledge SJ (The DNA damage response: ten years after. Mol Cell 28:739-745.2007).
Hengartner MO (The biochemistry of apoptosis. Nature 407:770-776.2000).

Higashitani A, Aoki H, Mori A, Sasagawa Y, Takanami T, Takahashi H (Caenorhabditis elegans Chk2-like gene is essential for meiosis but dispensable for DNA repair. FEBS Lett 485:35-39.2000).

Hoglinger GU, Breunig JJ, Depboylu C, Rouaux C, Michel PP, Alvarez-Fischer D, Boutillier AL, Degregori J, Oertel WH, Rakic P, Hirsch EC, Hunot S (The pRb/E2F cell-cycle pathway mediates cell death in Parkinson's disease. Proc Natl Acad Sci U S A 104:3585-3590.2007).

Ishii N, Fujii M, Hartman PS, Tsuda M, Yasuda K, Senoo-Matsuda N, Yanase S, Ayusawa D, Suzuki K (A mutation in succinate dehydrogenase cytochrome b causes oxidative stress and ageing in nematodes. Nature 394:694-697.1998).

Ishimura R, Martin GR, Ackerman SL (Loss of apoptosis-inducing factor results in cell-type-specific neurogenesis defects. J Neurosci 28:4938-4948.2008).

Itoh K, Tamura Y, Iijima M, Sesaki H (Effects of Fcj1-Mos1 and mitochondrial division on aggregation of mitochondrial DNA nucleoids and organelle morphology. Mol Biol Cell 24:1842-1851.2013).

Jaattela M, Tschopp J (Caspase-independent cell death in T lymphocytes. Nat Immunol 4:416-423.2003).

Jacobson MD, Burne JF, Raff MC (Programmed cell death and Bcl-2 protection in the absence of a nucleus. EMBO J 13:1899-1910.1994).

Joza N, Oudit GY, Brown D, Benit P, Kassiri Z, Vahsen N, Benoit L, Patel MM, Nowikovsky K, Vassault A, Backx PH, Wada T, Kroemer G, Rustin P, Penninger JM (Muscle-specific loss of apoptosis-inducing factor leads to mitochondrial dysfunction, skeletal muscle atrophy, and dilated cardiomyopathy. Mol Cell Biol 25:10261-10272.2005).

Joza N, Susin SA, Daugas E, Stanford WL, Cho SK, Li CY, Sasaki T, Elia AJ, Cheng HY, Ravagnan L, Ferri KF, Zamzami N, Wakeham A, Hakem R, Yoshida H, Kong YY, Mak TW, Zuniga-Pflucker JC, Kroemer G, Penninger JM (Essential role of the mitochondrial apoptosis-inducing factor in programmed cell death. Nature 410:549-554.2001).

Juo P, Harbaugh T, Garriga G, Kaplan JM (CDK-5 regulates the abundance of GLR-1 glutamate receptors in the ventral cord of Caenorhabditis elegans. Mol Biol Cell 18:3883-3893.2007).

Kadyk LC, Kimble J (Genetic regulation of entry into meiosis in Caenorhabditis elegans. Development 125:1803-1813.1998).

Kageyama Y, Hoshijima M, Seo K, Bedja D, Sysa-Shah P, Andrabi SA, Chen W, Hoke A, Dawsn VL, Dawson TM, Gabrielson K, Kass DA, Iijima M, Sesaki H (Parkin-independent mitophagy requires Drp1 and maintains the integrity of mammalian heart and brain. EMBO J.2014).

Kageyama Y, Zhang Z, Roda R, Fukaya M, Wakabayashi J, Wakabayashi N, Kensler TW, Reddy PH, Iijima M, Sesaki H (Mitochondrial division ensures the survival of postmitotic neurons by suppressing oxidative damage. J Cell Biol 197:535-551.2012).

Kamath RS, Fraser AG, Dong Y, Poulin G, Durbin R, Gotta M, Kanapin A, Le Bot N, Moreno S, Sohrmann M, Welchman DP, Zipperlen P, Ahringer J (Systematic functional analysis of the Caenorhabditis elegans genome using RNAi. Nature 421:231-237.2003).

Kayser EB, Morgan PG, Hoppel CL, Sedensky MM (Mitochondrial expression and function of GAS-1 in Caenorhabditis elegans. J Biol Chem 276:20551-20558.2001).

Kayser EB, Sedensky MM, Morgan PG, Hoppel CL (Mitochondrial oxidative phosphorylation is defective in the long-lived mutant clk-1. J Biol Chem 279:54479-54486.2004).

Kipreos ET (C. elegans cell cycles: invariance and stem cell divisions. Nat Rev Mol Cell Biol 6:766-776.2005).

Klein JA, Longo-Guess CM, Rossmann MP, Seburn KL, Hurd RE, Frankel WN, Bronson RT, Ackerman SL (The harlequin mouse mutation downregulates apoptosis-inducing factor. Nature 419:367-374.2002).

Koopman WJ, Distelmaier F, Smeitink JA, Willems PH (OXPHOS mutations and neurodegeneration. EMBO J 32:9-29.2013).

Lee HC, Yin PH, Lu CY, Chi CW, Wei YH (Increase of mitochondria and mitochondrial DNA in response to oxidative stress in human cells. Biochem J 348 Pt 2:425-432.2000).
Lee SS, Lee RY, Fraser AG, Kamath RS, Ahringer J, Ruvkun G (A systematic RNAi screen identifies a critical role for mitochondria in C. elegans longevity. Nat Genet 33:40-48.2003).
Leist M, Jaattela M (Four deaths and a funeral: from caspases to alternative mechanisms. Nat Rev Mol Cell Biol 2:589-598.2001).
Liesa M, Palacin M, Zorzano A (Mitochondrial dynamics in mammalian health and disease. Physiol Rev 89:799-845.2009).
Lill R, Muhlenhoff U (Maturation of iron-sulfur proteins in eukaryotes: mechanisms, connected processes, and diseases. Annu Rev Biochem 77:669-700.2008).
Liu L, Xing D, Chen WR (Micro-calpain regulates caspase-dependent and apoptosis inducing factor-mediated caspase-independent apoptotic pathways in cisplatin-induced apoptosis. Int J Cancer 125:2757-2766.2009).
Livak KJ, Schmittgen TD (Analysis of relative gene expression data using real-time quantitative PCR and the 2(-Delta Delta C(T)) Method. Methods 25:402-408.2001).
Lopes JP, Agostinho P (Cdk5: multitasking between physiological and pathological conditions. Prog Neurobiol 94:49-63.2011).
Lopes JP, Oliveira CR, Agostinho P (Cdk5 acts as a mediator of neuronal cell cycle re-entry triggered by amyloid-beta and prion peptides. Cell Cycle 8:97-104.2009).
Lopes JP, Oliveira CR, Agostinho P (Neurodegeneration in an Abeta-induced model of Alzheimer's disease: the role of Cdk5. Aging Cell 9:64-77.2010).
Lorenzo HK, Susin SA, Penninger J, Kroemer G (Apoptosis inducing factor (AIF): a phylogenetically old, caspase-independent effector of cell death. Cell Death Differ 6:516-524.1999).
Malka F, Lombes A, Rojo M (Organization, dynamics and transmission of mitochondrial DNA: focus on vertebrate nucleoids. Biochim Biophys Acta 1763:463-472.2006).
Mate MJ, Ortiz-Lombardia M, Boitel B, Haouz A, Tello D, Susin SA, Penninger J, Kroemer G, Alzari PM (The crystal structure of the mouse apoptosis-inducing factor AIF. Nat Struct Biol 9:442-446.2002).
McDermott-Roe C, Ye J, Ahmed R, Sun XM, Serafin A, Ware J, Bottolo L, Muckett P, Canas X, Zhang J, Rowe GC, Buchan R, Lu H, Braithwaite A, Mancini M, Hauton D, Marti R, Garcia-Arumi E, Hubner N, Jacob H, Serikawa T, Zidek V, Papousek F, Kolar F, Cardona M, Ruiz-Meana M, Garcia-Dorado D, Comella JX, Felkin LE, Barton PJ, Arany Z, Pravenec M, Petretto E, Sanchis D, Cook SA (Endonuclease G is a novel determinant of cardiac hypertrophy and mitochondrial function. Nature 478:114-118.2011).
Miquel J, Economos AC, Fleming J, Johnson JE, Jr. (Mitochondrial role in cell aging. Exp Gerontol 15:575-591.1980).
Miramar MD, Costantini P, Ravagnan L, Saraiva LM, Haouzi D, Brothers G, Penninger JM, Peleato ML, Kroemer G, Susin SA (NADH oxidase activity of mitochondrial apoptosis-inducing factor. J Biol Chem 276:16391-16398.2001).
Mori C, Takanami T, Higashitani A (Maintenance of mitochondrial DNA by the Caenorhabditis elegans ATR checkpoint protein ATL-1. Genetics 180:681-686.2008).
Nakada K, Sato A, Hayashi J (Mitochondrial functional complementation in mitochondrial DNA-based diseases. Int J Biochem Cell Biol 41:1907-1913.2009).
Narendra D, Tanaka A, Suen DF, Youle RJ (Parkin is recruited selectively to impaired mitochondria and promotes their autophagy. J Cell Biol 183:795-803.2008).
Neuspiel M, Schauss AC, Braschi E, Zunino R, Rippstein P, Rachubinski RA, Andrade-Navarro MA, McBride HM (Cargo-selected transport from the mitochondria to peroxisomes is mediated by vesicular carriers. Curr Biol 18:102-108.2008).
Newmeyer DD, Farschon DM, Reed JC (Cell-free apoptosis in Xenopus egg extracts: inhibition by Bcl-2 and requirement for an organelle fraction enriched in mitochondria. Cell 79:353-364.1994).

Nguyen MD, Lariviere RC, Julien JP (Deregulation of Cdk5 in a mouse model of ALS: toxicity alleviated by perikaryal neurofilament inclusions. Neuron 30:135-147.2001).

Nicholls TJ, Minczuk M (In D-loop: 40 years of mitochondrial 7S DNA. Exp Gerontol 56:175-181.2014).

Nicholls TJ, Zsurka G, Peeva V, Scholer S, Szczesny RJ, Cysewski D, Reyes A, Kornblum C, Sciacco M, Moggio M, Dziembowski A, Kunz WS, Minczuk M (Linear mtDNA fragments and unusual mtDNA rearrangements associated with pathological deficiency of MGME1 exonuclease. Hum Mol Genet 23:6147-6162.2014).

Nishimura Y, Yoshinari T, Naruse K, Yamada T, Sumi K, Mitani H, Higashiyama T, Kuroiwa T (Active digestion of sperm mitochondrial DNA in single living sperm revealed by optical tweezers. Proc Natl Acad Sci U S A 103:1382-1387.2006).

Odajima J, Wills ZP, Ndassa YM, Terunuma M, Kretschmannova K, Deeb TZ, Geng Y, Gawrzak S, Quadros IM, Newman J, Das M, Jecrois ME, Yu Q, Li N, Bienvenu F, Moss SJ, Greenberg ME, Marto JA, Sicinski P (Cyclin E constrains Cdk5 activity to regulate synaptic plasticity and memory formation. Dev Cell 21:655-668.2011).

Ohsato T, Ishihara N, Muta T, Umeda S, Ikeda S, Mihara K, Hamasaki N, Kang D (Mammalian mitochondrial endonuclease G. Digestion of R-loops and localization in intermembrane space. Eur J Biochem 269:5765-5770.2002).

Parashos SA, Luo S, Biglan KM, Bodis-Wollner I, He B, Liang GS, Ross GW, Tilley BC, Shulman LM (Measuring disease progression in early Parkinson disease: the National Institutes of Health Exploratory Trials in Parkinson Disease (NET-PD) experience. JAMA Neurol 71:710-716.2014).

Pohjoismaki JL, Goffart S (Of circles, forks and humanity: Topological organisation and replication of mammalian mitochondrial DNA. Bioessays 33:290-299.2011).

Polster BM, Basanez G, Etxebarria A, Hardwick JM, Nicholls DG (Calpain I induces cleavage and release of apoptosis-inducing factor from isolated mitochondria. J Biol Chem 280:6447-6454.2005).

Portt L, Norman G, Clapp C, Greenwood M, Greenwood MT (Anti-apoptosis and cell survival: a review. Biochim Biophys Acta 1813:238-259.2011).

Pospisilik JA, Knauf C, Joza N, Benit P, Orthofer M, Cani PD, Ebersberger I, Nakashima T, Sarao R, Neely G, Esterbauer H, Kozlov A, Kahn CR, Kroemer G, Rustin P, Burcelin R, Penninger JM (Targeted deletion of AIF decreases mitochondrial oxidative phosphorylation and protects from obesity and diabetes. Cell 131:476-491.2007).

Puigserver P, Spiegelman BM (Peroxisome proliferator-activated receptor-gamma coactivator 1 alpha (PGC-1 alpha): transcriptional coactivator and metabolic regulator. Endocr Rev 24:78-90.2003).

Rambold AS, Kostelecky B, Elia N, Lippincott-Schwartz J (Tubular network formation protects mitochondria from autophagosomal degradation during nutrient starvation. Proc Natl Acad Sci U S A 108:10190-10195.2011).

Riemer J, Fischer M, Herrmann JM (Oxidation-driven protein import into mitochondria: Insights and blind spots. Biochim Biophys Acta 1808:981-989.2011).

Rinaldi C, Grunseich C, Sevrioukova IF, Schindler A, Horkayne-Szakaly I, Lamperti C, Landoure G, Kennerson ML, Burnett BG, Bonnemann C, Biesecker LG, Ghezzi D, Zeviani M, Fischbeck KH (Cowchock syndrome is associated with a mutation in apoptosis-inducing factor. Am J Hum Genet 91:1095-1102.2012).

Rottenberg H, Scarpa A (Calcium uptake and membrane potential in mitochondria. Biochemistry 13:4811-4817.1974).

Ryan MT, Wagner R, Pfanner N (The transport machinery for the import of preproteins across the outer mitochondrial membrane. Int J Biochem Cell Biol 32:13-21.2000).

Saleem A, Hood DA (Acute exercise induces tumour suppressor protein p53 translocation to the mitochondria and promotes a p53-Tfam-mitochondrial DNA complex in skeletal muscle. J Physiol 591:3625-3636.2013).

Schagger H, de Coo R, Bauer MF, Hofmann S, Godinot C, Brandt U (Significance of respirasomes for the assembly/stability of human respiratory chain complex I. J Biol Chem 279:36349-36353.2004).

Schapira AH (Mitochondrial diseases. Lancet 379:1825-1834.2012).

Schulze-Osthoff K, Walczak H, Droge W, Krammer PH (Cell nucleus and DNA fragmentation are not required for apoptosis. J Cell Biol 127:15-20.1994).

Schweichel JU, Merker HJ (The morphology of various types of cell death in prenatal tissues. Teratology 7:253-266.1973).

Sevrioukova IF (Apoptosis-inducing factor: structure, function, and redox regulation. Antioxid Redox Signal 14:2545-2579.2011).

Sgarbi G, Matarrese P, Pinti M, Lanzarini C, Ascione B, Gibellini L, Dika E, Patrizi A, Tommasino C, Capri M, Cossarizza A, Baracca A, Lenaz G, Solaini G, Franceschi C, Malorni W, Salvioli S (Mitochondria hyperfusion and elevated autophagic activity are key mechanisms for cellular bioenergetic preservation in centenarians. Aging (Albany NY) 6:296-310.2014).

Sherr CJ (G1 phase progression: cycling on cue. Cell 79:551-555.1994).

Shi Y, Dierckx A, Wanrooij PH, Wanrooij S, Larsson NG, Wilhelmsson LM, Falkenberg M, Gustafsson CM (Mammalian transcription factor A is a core component of the mitochondrial transcription machinery. Proc Natl Acad Sci U S A 109:16510-16515.2012).

Short KR, Bigelow ML, Kahl J, Singh R, Coenen-Schimke J, Raghavakaimal S, Nair KS (Decline in skeletal muscle mitochondrial function with aging in humans. Proc Natl Acad Sci U S A 102:5618-5623.2005).

Song Z, Ghochani M, McCaffery JM, Frey TG, Chan DC (Mitofusins and OPA1 mediate sequential steps in mitochondrial membrane fusion. Mol Biol Cell 20:3525-3532.2009).

Soubannier V, McLelland GL, Zunino R, Braschi E, Rippstein P, Fon EA, McBride HM (A vesicular transport pathway shuttles cargo from mitochondria to lysosomes. Curr Biol 22:135-141.2012a).

Soubannier V, Rippstein P, Kaufman BA, Shoubridge EA, McBride HM (Reconstitution of mitochondria derived vesicle formation demonstrates selective enrichment of oxidized cargo. PLoS One 7:e52830.2012b).

Suetomi K, Mereiter S, Mori C, Takanami T, Higashitani A (Caenorhabditis elegans ATR checkpoint kinase ATL-1 influences life span through mitochondrial maintenance. Mitochondrion 13:729-735.2013).

Sugimoto T, Mori C, Takanami T, Sasagawa Y, Saito R, Ichiishi E, Higashitani A (Caenorhabditis elegans par2.1/mtssb-1 is essential for mitochondrial DNA replication and its defect causes comprehensive transcriptional alterations including a hypoxia response. Exp Cell Res 314:103-114.2008).

Suliman HB, Carraway MS, Piantadosi CA (Postlipopolysaccharide oxidative damage of mitochondrial DNA. Am J Respir Crit Care Med 167:570-579.2003).

Sumitani M, Kasashima K, Matsugi J, Endo H (Biochemical properties of Caenorhabditis elegans HMG-5, a regulator of mitochondrial DNA. J Biochem 149:581-589.2011).

Sun Y, Zhang Y, Wang X, Blomgren K, Zhu C (Apoptosis-inducing factor downregulation increased neuronal progenitor, but not stem cell, survival in the neonatal hippocampus after cerebral hypoxia-ischemia. Mol Neurodegener 7:17.2012).

Susin SA, Lorenzo HK, Zamzami N, Marzo I, Snow BE, Brothers GM, Mangion J, Jacotot E, Costantini P, Loeffler M, Larochette N, Goodlett DR, Aebersold R, Siderovski DP, Penninger JM, Kroemer G (Molecular characterization of mitochondrial apoptosis-inducing factor. Nature 397:441-446.1999).

Susin SA, Zamzami N, Castedo M, Hirsch T, Marchetti P, Macho A, Daugas E, Geuskens M, Kroemer G (Bcl-2 inhibits the mitochondrial release of an apoptogenic protease. J Exp Med 184:1331-1341.1996).

Sutovsky P, Moreno RD, Ramalho-Santos J, Dominko T, Simerly C, Schatten G (Ubiquitin tag for sperm mitochondria. Nature 402:371-372.1999).

Szczesny RJ, Hejnowicz MS, Steczkiewicz K, Muszewska A, Borowski LS, Ginalski K, Dziembowski A (Identification of a novel human mitochondrial endo-/exonuclease Ddk1/c20orf72 necessary for maintenance of proper 7S DNA levels. Nucleic Acids Res 41:3144-3161.2013).

Taylor RW, Turnbull DM (Mitochondrial DNA mutations in human disease. Nat Rev Genet 6:389-402.2005).

Trifunovic A, Hansson A, Wredenberg A, Rovio AT, Dufour E, Khvorostov I, Spelbrink JN, Wibom R, Jacobs HT, Larsson NG (Somatic mtDNA mutations cause aging phenotypes without affecting reactive oxygen species production. Proc Natl Acad Sci U S A 102:17993-17998.2005).

Twig G, Elorza A, Molina AJ, Mohamed H, Wikstrom JD, Walzer G, Stiles L, Haigh SE, Katz S, Las G, Alroy J, Wu M, Py BF, Yuan J, Deeney JT, Corkey BE, Shirihai OS (Fission and selective fusion govern mitochondrial segregation and elimination by autophagy. EMBO J 27:433-446.2008).

Urbano A, Lakshmanan U, Choo PH, Kwan JC, Ng PY, Guo K, Dhakshinamoorthy S, Porter A (AIF suppresses chemical stress-induced apoptosis and maintains the transformed state of tumor cells. EMBO J 24:2815-2826.2005).

Vahsen N, Cande C, Briere JJ, Benit P, Joza N, Larochette N, Mastroberardino PG, Pequignot MO, Casares N, Lazar V, Feraud O, Debili N, Wissing S, Engelhardt S, Madeo F, Piacentini M, Penninger JM, Schagger H, Rustin P, Kroemer G (AIF deficiency compromises oxidative phosphorylation. EMBO J 23:4679-4689.2004).

Vahsen N, Cande C, Dupaigne P, Giordanetto F, Kroemer RT, Herker E, Scholz S, Modjtahedi N, Madeo F, Le Cam E, Kroemer G (Physical interaction of apoptosis-inducing factor with DNA and RNA. Oncogene 25:1763-1774.2006).

van der Laan M, Bohnert M, Wiedemann N, Pfanner N (Role of MINOS in mitochondrial membrane architecture and biogenesis. Trends Cell Biol 22:185-192.2012).

Wang X, Yang C, Chai J, Shi Y, Xue D (Mechanisms of AIF-mediated apoptotic DNA degradation in Caenorhabditis elegans. Science 298:1587-1592.2002).

Whelan SP, Zuckerbraun BS (Mitochondrial signaling: forwards, backwards, and in between. Oxid Med Cell Longev 2013:351613.2013).

Wohlrab H (Transport proteins (carriers) of mitochondria. IUBMB Life 61:40-46.2009).

Yang W, Hekimi S (A mitochondrial superoxide signal triggers increased longevity in Caenorhabditis elegans. PLoS Biol 8:e1000556.2010).

Yang YY, Gangoiti JA, Sedensky MM, Morgan PG (The effect of different ubiquinones on lifespan in Caenorhabditis elegans. Mech Ageing Dev 130:370-376.2009).

Ye H, Cande C, Stephanou NC, Jiang S, Gurbuxani S, Larochette N, Daugas E, Garrido C, Kroemer G, Wu H (DNA binding is required for the apoptogenic action of apoptosis inducing factor. Nat Struct Biol 9:680-684.2002).

Ylikallio E, Tyynismaa H, Tsutsui H, Ide T, Suomalainen A (High mitochondrial DNA copy number has detrimental effects in mice. Hum Mol Genet 19:2695-2705.2010).

Youle RJ, van der Bliek AM (Mitochondrial fission, fusion, and stress. Science 337:1062-1065.2012).

Yu SW, Wang Y, Frydenlund DS, Ottersen OP, Dawson VL, Dawson TM (Outer mitochondrial membrane localization of apoptosis-inducing factor: mechanistic implications for release. ASN Neuro 1.2009).

Yuste VJ, Moubarak RS, Delettre C, Bras M, Sancho P, Robert N, d'Alayer J, Susin SA (Cysteine protease inhibition prevents mitochondrial apoptosis-inducing factor (AIF) release. Cell Death Differ 12:1445-1448.2005).

Zamzami N, Marchetti P, Castedo M, Zanin C, Vayssiere JL, Petit PX, Kroemer G (Reduction in mitochondrial potential constitutes an early irreversible step of programmed lymphocyte death in vivo. J Exp Med 181:1661-1672.1995).

Zamzami N, Susin SA, Marchetti P, Hirsch T, Gomez-Monterrey I, Castedo M, Kroemer G (Mitochondrial control of nuclear apoptosis. J Exp Med 183:1533-1544.1996).

Zanna C, Ghelli A, Porcelli AM, Karbowski M, Youle RJ, Schimpf S, Wissinger B, Pinti M, Cossarizza A, Vidoni S, Valentino ML, Rugolo M, Carelli V (OPA1 mutations associated with dominant optic atrophy impair oxidative phosphorylation and mitochondrial fusion. Brain 131:352-367.2008).

Zhang J, Cicero SA, Wang L, Romito-Digiacomo RR, Yang Y, Herrup K (Nuclear localization of Cdk5 is a key determinant in the postmitotic state of neurons. Proc Natl Acad Sci U S A 105:8772-8777.2008).

Zhang J, Li H, Yabut O, Fitzpatrick H, D'Arcangelo G, Herrup K (Cdk5 suppresses the neuronal cell cycle by disrupting the E2F1-DP1 complex. J Neurosci 30:5219-5228.2010).

## 9. Acknowledgement

First I would like to thank Professor Nicotera for giving me the opportunity to start my PhD thesis in his lab and for his mentorship during the course of my work. Moreover, I thank Dr. Daniele Bano for supervising me and for the trust he placed in my work during the past few years. Additionally, I want to thank Professor Hoch for his support and for helping me to set up the administrative framework to become the first PhD student in the DZNE. I kindly thank Professors Bradke and von der Emde for graciously consenting to be part of my thesis committee.

Moreover, I thank Sarah, Anastasia, Antonia and Jörg for the critical comments on my thesis.

I am deeply grateful to the former and present members in the group; you created a fun and warm atmosphere in the lab! Thanks to Christiane and Banu for supporting my work with their helping hands. Miriam, I am very grateful for your help with the mice and of course for being such a great team player with the lab organization. I thank you and Alessandra for helping me with all the mice related issues. Simona and Ylva, I am grateful that you always had an open ear for me. Anastasia, I have to thank you for jumping on the fitness train and for the motivation in this respect, we went through many fitness adventures and we learned how to dig deeper in our bootcamp sessions. Sven, thank you for all the scientific and non-scientific discussions we had, for all the laughter, moronic games and practical jokes; of course I am impressed that you are still that pretty.

Natürlich möchte ich mich bei meiner Familie bedanken, ohne euch wäre diese Arbeit nicht möglich gewesen. Danke, dass ihr immer für mich da seid. Danke, dass ihr mir zuhört und mich aufmuntert. Danke für eure Ratschläge und euer Vertrauen.

Zu Schluss bedanke ich mich bei meinem Jörg für so vieles! Danke für die Unterstützung in schwierigen Zeiten und den besten Gin Tonic der Welt.